SOME APPLICATIONS OF A SVEDBERG ROTOR

IN

ULTRACENTRIFUGE MEASUREMENTS

A Thesis Submitted to the Faculty
of Graduate Studies and Research
of McGill University, in partial
fulfilment of the Requirements for
the Degree of Doctor of Philosophy

by

Robert C. Gunton, M.A.

The Macdonald Physics Laboratory,
McGill University. September, 1947.

ACKNOWLEDGEMENT

Sincere thanks are due to Professor J. S. Foster for suggesting the ultracentrifuge problem to the writer, and for his interest and support during the course of the work.

Professor C. A. Winkler of the Chemistry Department, and Dr. J. S. Tapp of the Research and Development Division of the Polymer Corporation, suggested applications of the ultracentrifuge, and gave valuable advice.

Grateful acknowledgement must be made to Mr. J. A. Massé, of the Radiation Laboratory staff, for much assistance and advice with the machining of parts.

Mr. J. Alex Carruthers collaborated with the writer at various stages and rendered invaluable assistance.

Mrs. V. Clarke, Mr. M. Gransden, Mr. L. Newsham, and Mr. R. Sharpe gave technical aid.

The writer is greatly indebted, also, to the National Research Council for the award of two Studentships during the research period.

SUMMARY

A Svedberg rotor and an optical system, including a quartz spectrograph, have been constructed for use with an electrically driven ultracentrifuge.

An electronic speed control allows acceleration of the rotor to a predetermined speed and maintains the speed constant to within 0.1%

A value obtained for the sedimentation constant of egg albumin, 3.8×10^{-13} , shows agreement with the accepted value, 3.55×10^{-13}.

Preliminary experiments with 0.25% soap solutions reveal a slight sedimentation inward toward the meniscus in a centrifugal field of 150,000 g.

The weight-optical average particle radii of Types II and V GR-S synthetic rubber latices are found, by sedimentation velocity measurements in a field of 1960 g, to be 590 A° and 940 A°, respectively.

TABLE OF CONTENTS

TABLE OF CONTENTS (Continued)

I. INTRODUCTION

(a) Historical

The method of separating substances by centrifuging is so ancient that its origin is unrecorded. In recent years, its use has become more widespread until, today, centrifuges are employed in many industries and in most laboratories. However, the development of the technique of employing very high centrifugal fields for the measurement of particle sizes has taken place since 1923.

The measurement of the sedimentation velocity of particles in a fluid under the influence of gravity by Perrin[1], has yielded information about particle sizes. However, the application of the method is limited to particles of high density by the weakness of the earth's gravitational field. For the investigation of colloids and high molecular weight substances, much higher fields obviously were necessary.

Dumansky[2], in 1913, attempted to measure particle sizes by rotating solutions in ordinary laboratory centrifuges. The results obtained were in disagreement with ultramicroscopic values; the discrepancies are now known to be due to temperature gradients in the solutions.

Svedberg and Rinde[3], in 1923, decided from optical measurements on a gold colloid sedimenting in the gravitational field, that the size distribution of smaller colloidal particles might be

obtained from optical measurements on a rotating sample, if the latter could be maintained at a constant temperature.

Studies by Svedberg, Nichols and Rinde[4] revealed that, for convection-free sedimentation, the sample must be sector-shaped, small and completely enclosed. It must rotate in a friction-free medium and heat from the bearings must be removed. They obtained convection-free sedimentation in fields of 5000 times gravity (5000g) and proposed the name "ultracentrifuge" for the new research tool.

Since 1923, the work of Svedberg and his students has proceeded in two directions. One has led to the development of a stable, low-speed, electrically-driven ultracentrifuge with ball bearings, whose principal use is in sedimentation equilibrium measurements. The other has led to the production of very high centrifugal fields, suitable for sedimentation velocity measurements of high-molecular substances such as proteins.

These high fields are achieved in the "oil-turbine ultracentrifuge", a machine of marvellous design, in which a chrome-nickel steel rotor is supported in horizontal bearings and is spun by twin oil-turbines, one on each end of the shaft. The rotor is shaped for maximum rotational speed and carries a cell with transparent quartz windows. It rotates in an atmosphere of hydrogen, which has a low viscosity and high heat conductivity. A heavy steel casing surrounding the rotor is held at a constant temperature by circulating water.

With rotors having a cell radius of 6.5 cm., the rotational

speed was increased progressively to 77,000 RPM, at which the centrifugal field in the cell was 400,000 g. At greater speeds, the rotor material failed. Using smaller rotors, and finally with a cell radius of 3.2 cm., usable fields of 750,000 g. were produced at 148,000 RPM.

Another approach to the problem of producing high centrifugal fields has generated the air-driven ultracentrifuge. In 1925 Henriot and Huguenard[6] constructed a centrifuge of the spinning-top type, which was driven and supported by air jets. In its original form, the rotor had to be small for high speed operation and it did not seem useful for measurements. The rotor turned in air at atmospheric pressure; temperature control was difficult and high driving pressures were required for high rotational speeds.

The air-driven centrifuge has been developed by J. W. Beams[7-10] and his co-workers, with a view to overcoming the difficulties mentioned above. The final result is the vacuum-type air-driven centrifuge which has a large rotor situated inside an evacuated chamber, driven and supported by an air turbine located above the chamber. The rotor and turbine are connected by a flexible shaft which passes through a vacuum-tight oil bearing. The rotor seeks its own axis of rotation, owing to the flexibility of the shaft and is thus self-balancing. Convection-free sedimentation in a large rotor can be readily attained. Reverse jets on the turbine permit rapid deceleration.

Mention must be made of the work of McBain and his colleagues[11-15]

in the development of the directly air-driven top as an ultracentrifuge.

The control of rotational speed was difficult with the air-driven centrifuges. In ultracentrifuge measurements, a constant, known speed is essential. Beams and co-workers[16-18] have developed the electrically-driven vacuum ultracentrifuge, in which the air turbine is replaced by a small electric motor. The motor, usually an induction type, is driven by high frequency alternating currents and can be controlled accurately in speed. The air bearing support of the air turbine is replaced by a magnetic support consisting of a solenoid lifting upward on an extension of the rotating motor armature. The magnetic support permits rotational speeds as high as those with the air-bearing support. In the latest model of the electrically-driven ultracentrifuge, as developed by Skarstrom and Beams[18], an electronic speed control permits very great constancy of speed to be attained.

(b) Previous Work at McGill University

In 1937, Professor J. S. Foster and Dr. D. Shugar began the construction of a high-speed vacuum centrifuge. There were built a substantial vacuum chamber, a vacuum system, a quantity rotor and a Svedberg rotor similar to those described by Bauer and Pickels[19,20], and two cells for the Svedberg rotor[20]. Several types of air turbine drives, similar to those described by Bauer and Pickels[20] and by Pickels[21], were tried. Rotational speeds of 18,000 RPM with the quantity rotor and 30,000 RPM with the Svedberg rotor were

reached in 1940. The probable safe maximum speeds are 30,000 RPM and 60,000 RPM, respectively, for these rotors. They were not attained because of the limited capacity of the available air compressor. An electric drive, of a type described by Beams and Black[17] was partially completed when the details of a more satisfactory electric drive, that of Skarstrom and Beams[18] were received.

Dr. A. B. Rotenberg was assigned the problem of assembling the later electric drive and completed the work in August of 1941. During early trials with the new machine, a drive shaft became fatigued and broke, as a result of excessive precessional vibrations, when the Svedberg rotor was turning at 10,000 RPM. The rotor was damaged beyond repair and could not be replaced, owing to the unavailability of duralumin rotor material. Experiments were continued with the quantity rotor and eventually, when a satisfactory standard of performance of the machine was attained, the latter was applied in making an equilibrium measurement of the molecular weight of lignin and in testing the effect of high centrifugal fields on two types of plant cells.

During the later war years, the ultracentrifuge was not used. In late 1946, Professor Foster suggested that the writer recondition the machine and apply it to a suitable problem.

Since then, two new Svedberg rotors have been made, the optical system has been built, the vacuum system rebuilt, the speed control added and other changes enumerated below have been incorporated into the apparatus. Finally, the experimental work described below has been performed.

II. THE CONSTRUCTION OF THE ULTRACENTRIFUGE

The ultracentrifuge is essentially similar to that of Skarstrom and Beams[18], although it differs in many details. It is illustrated in Figure 1, a scale drawing, in section and in Photographs 1-4. The letters used in the description below refer to the scale drawing. Since the construction is described in considerable detail by Rotenberg[23], only the principal features will be mentioned below.

(a) The Rotating System

This consists of the armature and shaft assembly (parts S_1, Q, T, A, D, S_2) and the rotor R. The support core T, the motor armature A and parts Q and D are made of cold-rolled steel; whereas the upper and lower shafts S_1 and S_2 are stainless steel tubes, 1/8" in outer diameter.

The lower shaft S_2, fitted tightly into D, is secured by a pin, which is drilled through to leave an unobstructed hole in the driveshaft; the pin is necessary for safe support of the weight of the rotor. Cooling water flows through the hole in the armature and shafts, while they are rotating, and escapes through a small hole in S_2.

A light and flexible shaft allows the rotor to select its own axis of rotation, and obviates the necessity of careful dynamic balancing of the latter. However, care must be taken in machining

CROSS-SECTION OF THE ULTRACENTRIFUGE, TO SCALE

FIGURE 1

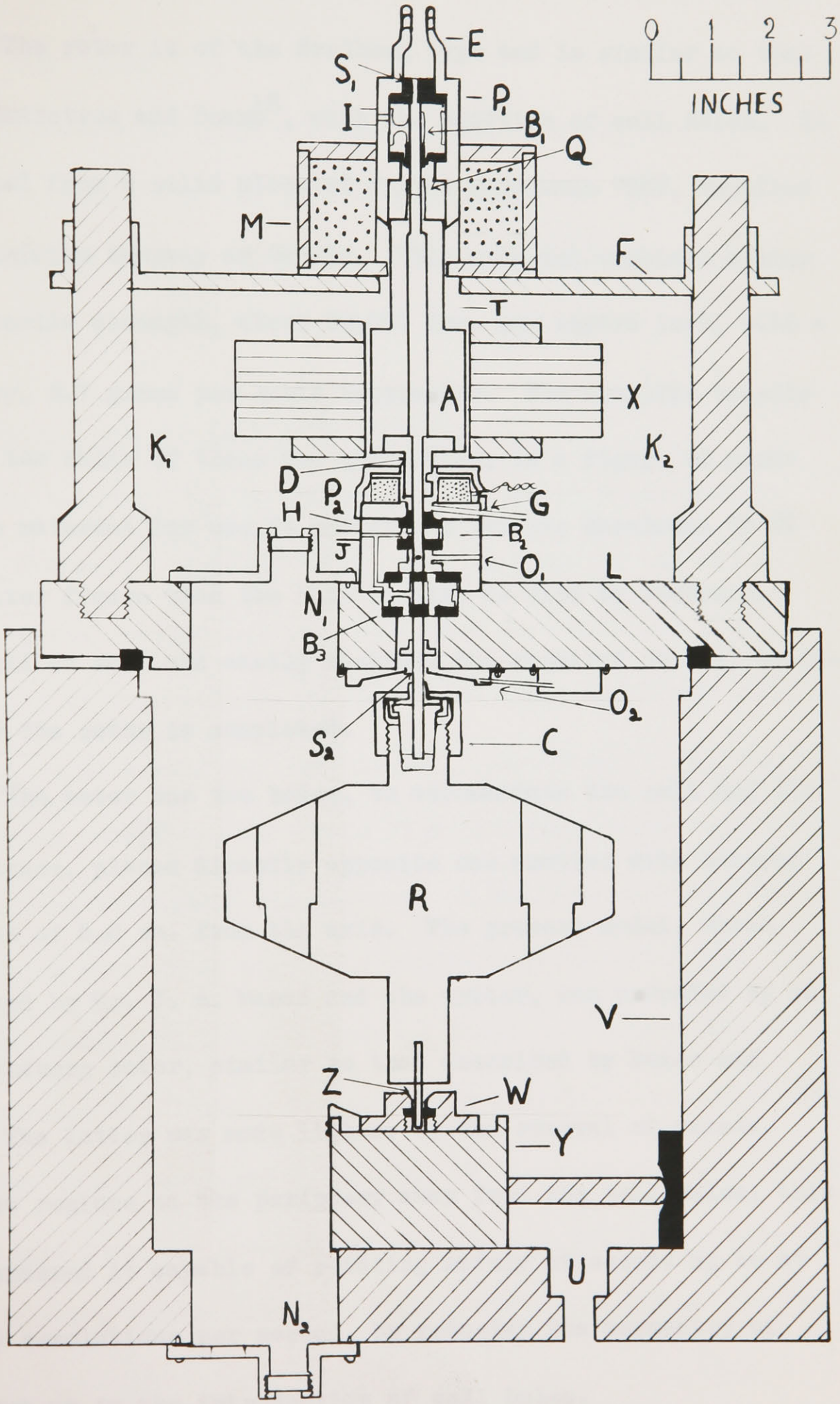
0 1 2 3
INCHES
E
S1
P1
I
B1
Q
M
F
T
A
X
K1
K2
D
P2
H
G
B2
J
O1
L
N1
B3
O2
S2
C
R
V
Z
W
Y
U
N2

the rotor to prevent the drive shaft, S_2, from being unduly fatigued by vibration.

The rotor is of the Svedberg type and is similar to that shown by Skarstrom and Beams[18], with the addition of cell holes. It was machined from a solid block of forged duralumin 75ST, supplied by the Aluminium Company of Canada. This material combines a high maximum tensile strength, about 82,000 lbs. per square inch, with a low density, 2.7 grams per cubic centimeter. The specific tensile strength, the ratio of these two quantities, is a figure of merit of a given material for use in centrifuge rotors; duralumin 75 ST has a greater figure than the best steels, as used by Svedberg. The material is soft and easily machined and requires no heat treatment after the rotor is completed.

The rotor has two holes, to accommodate the cell and its counterbalance, placed directly opposite one another with centres at a radius of 5.8 cm. from the axis. The present model, which was machined by Mr. J. A. Massé and the writer, was preceded by an earlier Svedberg rotor, similar to that described by Bauer and Pickels[20]. The latter was made lighter by the removal of excess material at regions on the periphery away from the cell holes; this process rendered it capable of rotating safely at speeds up to at least 1000 revolutions per second, by reducing the asymmetry of stresses set up in the introduction of cell holes.

Unfortunately, the earlier rotor was badly smashed when,

during the acceleration period prior to a run, the lower shaft fractured at the water outlet hole, while the speed of rotation was 600 revolutions per second.

The excess material was not removed from the present rotor, with a view to shortening the time of machining.

The rotor chuck, C, clamps the rotor firmly and centrally to the driveshaft.

(b) The Bearings and the Lubrication System.

The bearings B_1, B_2 and B_3 are similar to those used by Skarstrom and Beams.[18] Made of brass, each bearing has two babbitt inserts which are drilled axially and reamed carefully until the shaft slides into them without forcing. The upper and lower inserts are threaded right-handed and left-handed, respectively, in order that the shafts, which always rotate in a clockwise direction viewed from above, tend to tighten the inserts. A small hole in the side of each bearing acts as an inlet for the lubricating oil. The bearings are clamped in position between neoprene washers, which seal them against oil leakage and provide a somewhat flexible mounting.

Two lower bearings, B_2 and B_3,are necessary to allow cooling water to escape from the rotating system through the outlet tube, O_1. Bearing B_3 forms a vacuum seal where the drive shaft enters the vacuum chamber.

The bearings are lubricated by Hyvac pump oil, a low vapor pressure oil forced in, under pressure from a reservoir, at oil in-

lets I and J. For continuous lubrication, oil must leak from the outer ends of the babbitts. The writer found it necessary to add collectors for the oil escaping from the lower babbitt of B_1, the upper babbitt of B_2, and the lower babbitt of B_3. Those for the latter two bearings are shown in Figure 1. The oil collector O_2 for B_3 is essential to prevent oil from reaching the rotor cell hole. Properly fitting bearings experience a leakage of about 2 c.c. per hour from each babbitt.

(c) The Magnetic Support

The solenoid M carries most of the weight of the rotating system by lifting on the support core T; the remainder of the weight is exerted by D on the upper babbitt of B_2. The solenoid pole piece is symmetrical about T; hence there is little drag on T due to eddy currents. The solenoid winding, which is encased in steel, is energized by two six-volt storage batteries in series. A series adjusting rheostat and an ammeter, both mounted on the control panel, permit setting the current to the required value. The writer found it necessary to "float" the batteries on the 110-volt D.C. line, with a series charging resistor, in order to prevent the solenoid current from decreasing during a run. In operation, the solenoid began to raise the rotating system with a current of 2.45 amperes.

(d) The Induction Motor

The laminated stator has four salient poles on which the stator coils are wound. A hole in the stator at a distance of 5.8 cm.

from the axis of rotation, allows light from the optical system to pass. The stator rests on three brass rods (not shown), which are screwed into the lid, L, of the vacuum chamber. Electrical connections to the motor are described below.

(e) The Vacuum System

Temperature gradients in the rotor must be avoided for convection-free sedimentation. The heat produced by friction of the rotor with a surrounding atmosphere may be eliminated by spinning the rotor in a high vacuum or in an atmosphere of hydrogen at 2 mm. pressure. The latter method is employed by Svedberg in the oil-turbine ultracentrifuge; the former is used in the McGill machine.

The vanadium steel vacuum chamber, V, is stoutly constructed and is more than ample for the protection of the operator in case the rotor explodes or a drive-shaft breaks. Rectangular holes, cut in the chamber lid, L, and in the bottom of the chamber are covered by the window supports, N_1 and N_2, of the optical system. A rubber gasket, 3/16" in thickness, fitted into an annular groove in the chamber lid, forms a vacuum seal when the lid is bolted to the chamber. Three stout, short legs, cast as part of the vacuum chamber, fit into short lengths of iron pipe. The latter are imbedded in a large block of concrete, built up from the floor of the room. Rubber washers, placed between the chamber legs and the pipes, serve to minimize the transmission of vibrations from the vacuum chamber to the floor, and thus to prevent vibration of the optical system.

The hole, U, in the bottom of the chamber, leads to the vacuum system. A Distillation Products oil diffusion pump of metal construction has been added to the original vacuum system, which consisted of a Cenco Megavac rotary pump and a McLeod gauge. In addition, the tube connecting the vacuum pumps to the chamber has been enlarged in diameter and reduced in length to increase its pumping speed as much as feasible. The Megavac pump alone produces a vacuum of 20 microns; the diffusion pump with a rated pumping speed of 10 litres per second, lowers the pressure to a value below one micron, which is the lower limit of the McLeod gauge range. In operation, the friction caused by this vacuum produces a negligible temperature rise in the rotor, even after several hours at a high rotational speed.

(f) Vibration Damping

The damping bearing, W and Y, modelled after that of Skarstrom and Beams[18], damps precessional vibrations of the rotor, which occur at various frequencies in the range from 6,000 RPM to 15,000 RPM. The bearing consists of an upper brass piece, W, which slides very freely on a firm brass base, Y. The spindle, Z, in the bottom stem of the rotor, projects into a hole in W and is centred in the latter by a leather washer, in which it can turn freely. A conical opening in the upper surface of W facilitates the entry of Z. Three springs, attached to Y, hold W in firm contact. The inertia of the system restricts the movement of the bottom stem of the rotor, and hence damps the intensity of precessional vibrations.

DRIVE CIRCUIT AND SLIP SPEED CONTROL

FIGURE 2

DRIVE CIRCUIT AND SLIP SPEED CONTROL

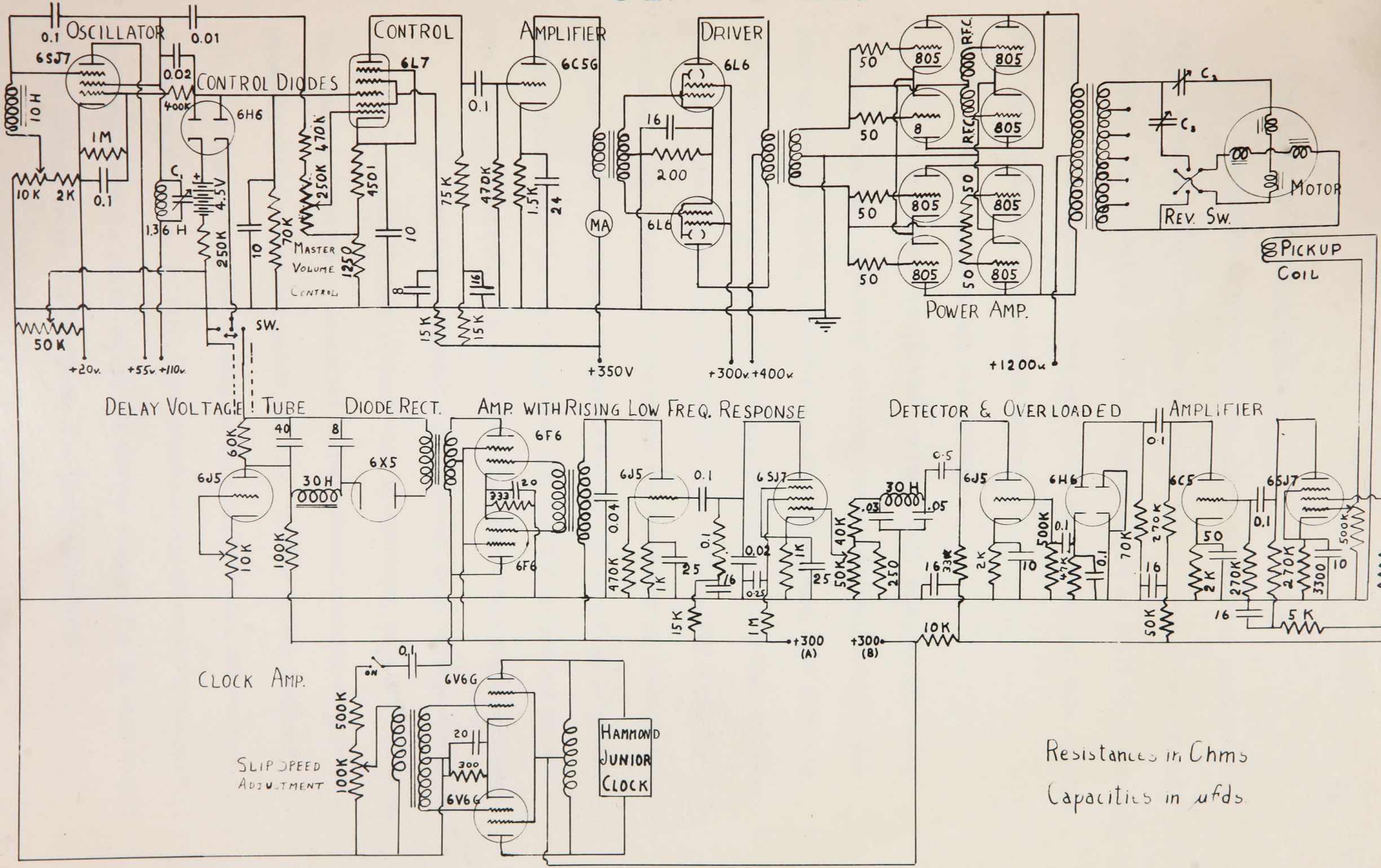

Resistances in Ohms
Capacities in ufds.

(g) The Electric Drive Circuits

The motor is driven by two phase alternating currents, obtained from an audio frequency generator with a power output of one kilowatt. The circuits, shown in Figure 2, are as built by Rotenberg, except for the addition by the writer of the 6L7 Control tube and the Slip Speed Control, as described below.

(i) The Audio Oscillator and Driver Stages:

A transitron oscillator,[22] using a 6SJ7 tube, is the audio frequency source. A delayed automatic volume control circuit, employing one 6H6 diode, prevents line voltage changes from altering the amplitude of the oscillator output voltage. A parallel resonant circuit, connected to the oscillator screen, consisting of C_1 and its associated inductance, determines the frequency of oscillation. The size of C_1 is altered in discrete steps by switching to provide twenty frequencies in the range from 430 to 1890 cycles per second. The oscillator output is 3 volts RMS throughout the frequency range.

The 6L7 Volume Control tube performs as a voltage amplifier for the oscillator output voltage and, in addition, as a control tube. The control function is described below. Manual control of gain is obtained with the potentiometer labelled "Master Volume Control".

The 6L7 output is coupled to a conventional 6C5 voltage amplifier which is, in turn, transformer--coupled to two push-pull 6L6's operating in class AB_1 as the driver stage. The 34 watt output of the latter drives the grids of the final amplifier.

All of these circuits are mounted on a small chassis, visible in Photograph 2, on the top of the control table.

The low voltage power supply for this unit, illustrated in Figure 3, is entirely conventional.

(ii) The Power Stage and the Motor:

The power stage must produce one kilowatt of audio power, if the acceleration time of the usual rotor is to be less than 30 minutes. This corresponds to a motor torque of 600 gm.-cm. In this stage, eight 805 triodes are employed in push-pull parallel, class B. At a plate voltage of 1250, their maximum rated output is 1200 watts.

The final output transformer couples the power tubes to the motor circuit. Depending on the frequency, the latter represents a load impedance in the range from 10 ohms to 2.5 ohms, which is matched to power stage by means of taps on the output transformer secondary.

The single phase output of the final stage is converted to two phases by the phase shifting condensers C_2 and C_3. The four windings of the motor are connected as two pairs to the two phases. The members of a pair are located opposite one another and are joined in series or in parallel, depending upon the impedance desired. The motor stator produces a rotating magnetic field through the tuning of one pair of stator coils above resonance with C_2 and the other below resonance with C_3, in such a way that the two currents are 90 degrees out of phase. C_2 and C_3 consist of banks of condensers whose members are selected, as desired, by switches.

POWER SUPPLIES

FIGURE 3

HIGH VOLTAGE POWER SUPPLY AND PROTECTIVE RELAY

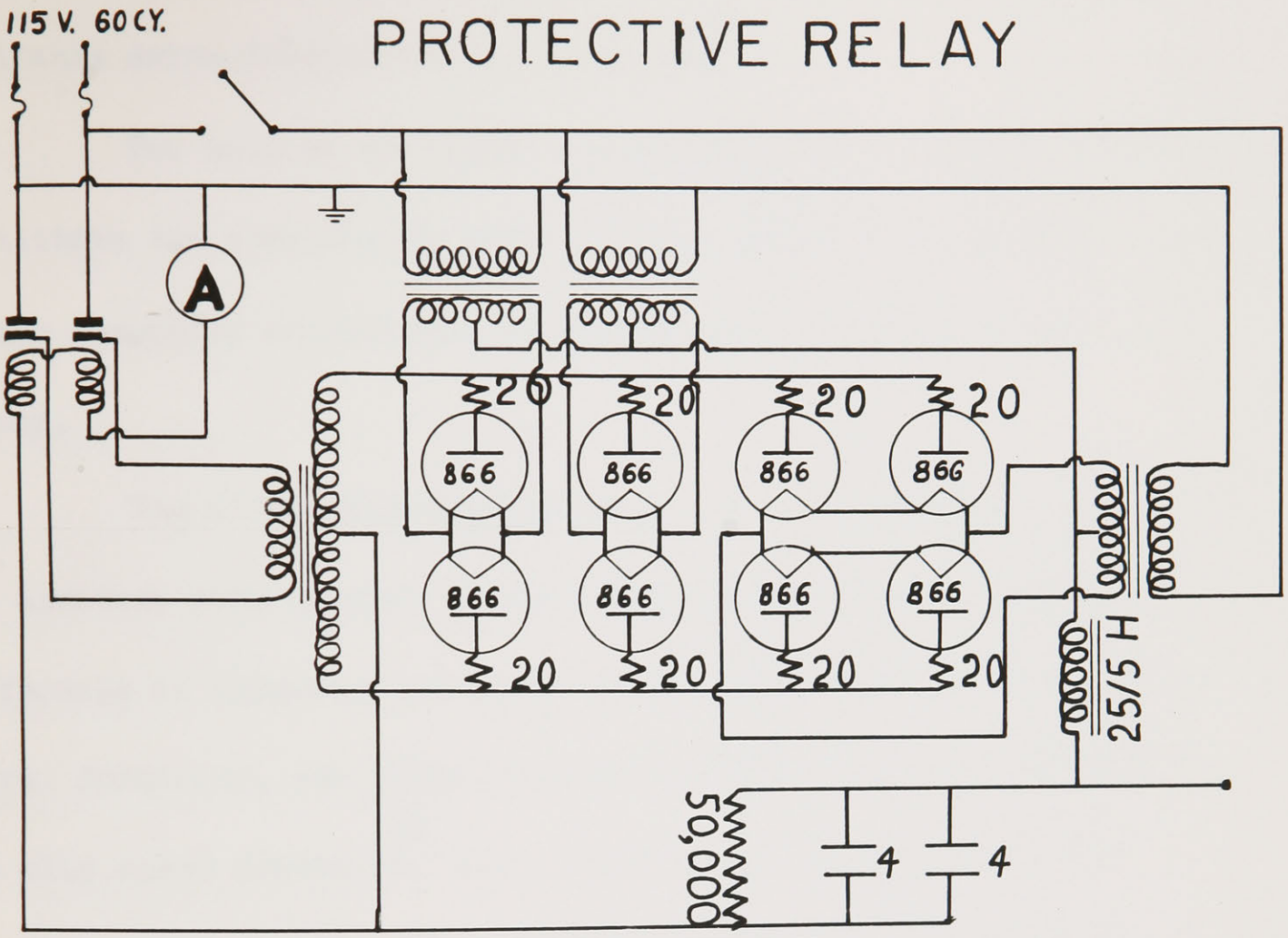

LOW VOLTAGE POWER SUPPLY

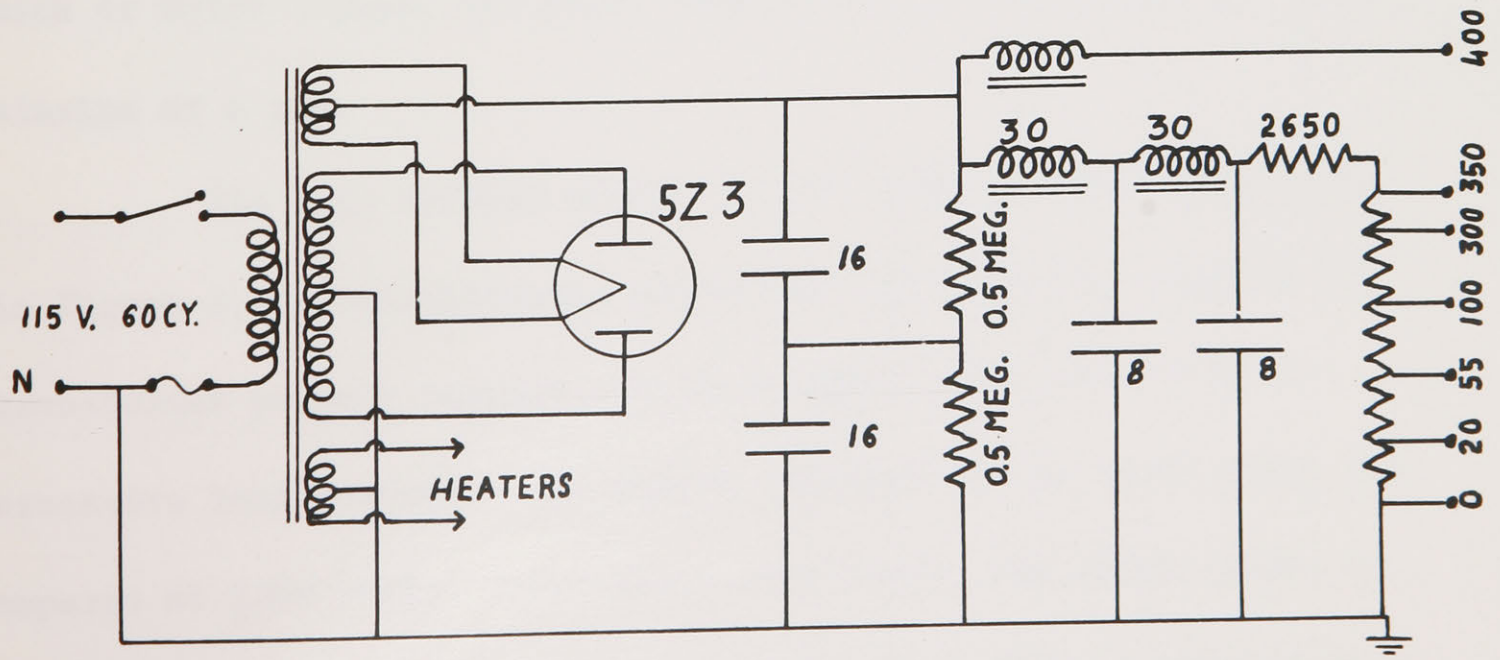

The optimum output transformer connections, phase shifting condenser values and motor connections, are tabulated for all of the available drive frequencies by Rotenberg.[23]

Two sets of switches, installed by Mr. J. Alex. Carruthers, facilitate the changing of motor stator connections and output transformer secondary connections in the event of a change of drive frequency.

The ultracentrifuge motor is not synchronous; a "slip" of the armature with respect to the drive frequency always occurs. The difference in frequency is known as the "slip speed". At a given drive frequency, the power required to turn the rotor increases as the slip speed decreases,[18] hence there is no possibility of the "running away", if the drive frequency is set at a safe value.

A reversing switch, shown in Figure 2, changes the direction of motor torque, for rapid deceleration of the rotor at the conclusion of a run.

The high voltage supply for the power stage, illustrated in Figure 3, is conventional, except for the overload relay in the transformer primary circuit, which is set to trip at a slightly excessive load current. The supply delivers to the power stage 1.5 amperes at 1200 volts, under which conditions, the power output is one kilowatt. The plate current to the power stage is metered on the control panel, illustrated in Photograph 2.

III. THE SLIP SPEED CONTROL

The slip speed control, built by the writer, is similar to but modified from that of Skarstrom and Beams[18], and is illustrated in Figure 2. It is actuated by a voltage from the pick-up coil, P_2 of Figure 1, placed about part D of the rotating assembly. The pick-up coil consists of 800 turns of No. 30 enamelled copper wire, wound on a brass spool. The latter is surrounded on top and on the sides by an iron sheath with 1/16" walls. The hole in the shield lid, through which the D passes, has the shape shown in Figure 7. In D at the height of the shield lid is a groove 3/32" wide, extending half-way around the shaft. The hole in the lid and the groove in the rotating shaft combine to modulate at the rotation frequency, the lines of force which pass axially along the shaft through the pick-up coil.

In the pick-up coil is induced a voltage having a component at the drive frequency as well as a component at the rotation frequency. The changing magnetic field of the motor stator coils produces the former; whereas interruption of the D.C. field of the supporting solenoid produces the latter. From this voltage, the difference frequency of these two components, or the slip frequency, may be produced by demodulation.

The pick-up coil voltage is applied to the input of a conventional audio amplifier consisting of two well-decoupled stages using 6SJ7 and 6C5 tubes. The 6C5 output voltage is coupled to a

6H6 half-wave diode detector, in whose load circuit arises a slip frequency voltage modulated by a drive frequency component. After amplification by an overloaded 6J5 triode stage, the detector output is applied to a single stage π low pass filter, having a cut-off frequency of 300 cycles per second. The filter attenuates greatly the drive frequency component. Overloading of the 6J5 stage eliminates the effect of variation of amplitude of the pick-up coil voltage. This portion of the circuit is essentially different from that of Skarstrom and Beams[18], who used plate detection rather than diode detection, and the selective property of a series resonant circuit instead of the low pass filter.

The slip frequency voltage is then coupled to the input of a three stage amplifier with a rising low frequency response. In the first two stages of voltage amplification using 6SJ7 and 6J5 tubes, bypass condensers at the plates attenuate the higher frequencies to produce the rising low frequency response. The output of the following push-pull 6F6 power amplifier is transformer-coupled to a 6X5 diode detector.circuit, on whose 60,000 ohm load resistor is produced a D.C. voltage which increases in amplitude as the slip frequency decreases.

A 6J5 delay tube produces a D.C. voltage between its plate and ground, which may be varied from 40 to 100 volts by means of the grid bias potentiometer labelled "Slip Speed Adjustment".

This delay voltage and the D.C. output voltage of the

amplifier with rising low frequency response are connected in series opposition to a diode detector using one half of a 6H6 tube. On the load resistor of this detector is produced a negative D.C. voltage only when the slip speed control voltage exceeds the delay voltage. This negative voltage varies the bias on grid No. 3 of the 6L7 Volume Control tube in the Drive Circuit. The fixed cathode bias on this grid is adjusted in order that any increase in negative bias from the control circuit decreases the transconductance of the 6L7 and hence reduces the audio power to the ultracentrifuge motor.

The action of the control is very sharp since an increase of one volt in the negative voltage at grid No. 3 of the 6L7 produces a decrease in the motor power of the order of 50%. The graph in Figure 4, showing the variation of speed with time during a 9-hour run at 800 revolutions per second, indicates a variation of speed of about $\pm 0.1\%$.

Speed measurements during this run were made with a General Radio Strobotac, whose flashing neon light illuminated a mark on part T of the rotating assembly. A simpler strobotac mounting directly on the side of the vacuum chamber has been built by Mr. J. Alex Carruthers. Illustrated in Photograph 3, it is calibrated over the range 5000 RPM to 20,000 RPM. Higher rotational speeds may be read by using a known sub-harmonic.

The slip speed adjustment may be calibrated in terms of slip speed, for a given drive frequency. Thus, the ultracentrifuge may be

SLIP SPEED CONTROL PERFORMANCE

FIGURE 4

SLIP SPEED CONTROL PERFORMANCE

SPEED - Revolutions per second.

0
200
400
600
800

801
800
799
798
797

In Change of Speed Scale

60 120 180 240 300 360 420 480 540

Time after Start - Minutes

accelerated automatically to a constant predetermined speed with no attention from the operator. Slip speeds are available in the range from 100 to 190 cycles per second.

The Clock Amplifier circuit of Figure 2 consists of two 6V6G tubes in push-pull driving a Hammond Junior electric clock at the slip frequency. The circuit acts as a means of reading the ultracentrifuge speed which is independent of the Strobotac method. The drive frequency, which must be used with the slip frequency for the calculation of the rotational speed, is known accurately because of the great frequency stability of the transitron oscillator circuit.

The power supply for the speed control (not illustrated) is conventional and consists of two units capable of supplying 300 volts D.C. at a current of 100 milliamperes.

Many thanks are due to Mrs. V. Clarke who assembled the control in its final form.

IV. THE OPTICAL SYSTEM

The optical system, illustrated in Figure 5, is used for the photographic recording of molecular sedimentation in the rotating solution, and is similar to those designed by Svedberg[5] for the oil-turbine ultracentrifuge.

Concentration distribution may be measured by employing either of two different properties of the solution; light absorption or refraction. At present only the light absorption method is used.

(a) The Cell

The material to be centrifuged is carried in a cell (Figure 6), which is similar to that described by Bauer and Pickels.[20] One of its essential components is the duralumin centrepiece, B, having a sector-shaped hole, F, of angular width 4 degrees with its apex at the axis of rotation (Figure 8). The sector shape is required in order that the particles or molecules may sediment unobstructed along radii, with an absence of stirring. The centrifugate is contained in this space which is of thickness 0.5 cm. and bounded by transparent quartz discs. The surfaces of the latter are parallel to the plane of rotation, so as to make possible photographic observations. The discs are made of crystalline quartz, with the optic axis perpendicular to the surfaces; they are of outer diameter 1.9 cm. and have a thickness of 0.5 cm.

The length of the cell space is 1.5 cm. a value found by

OPTICAL SYSTEM

FIGURE 5

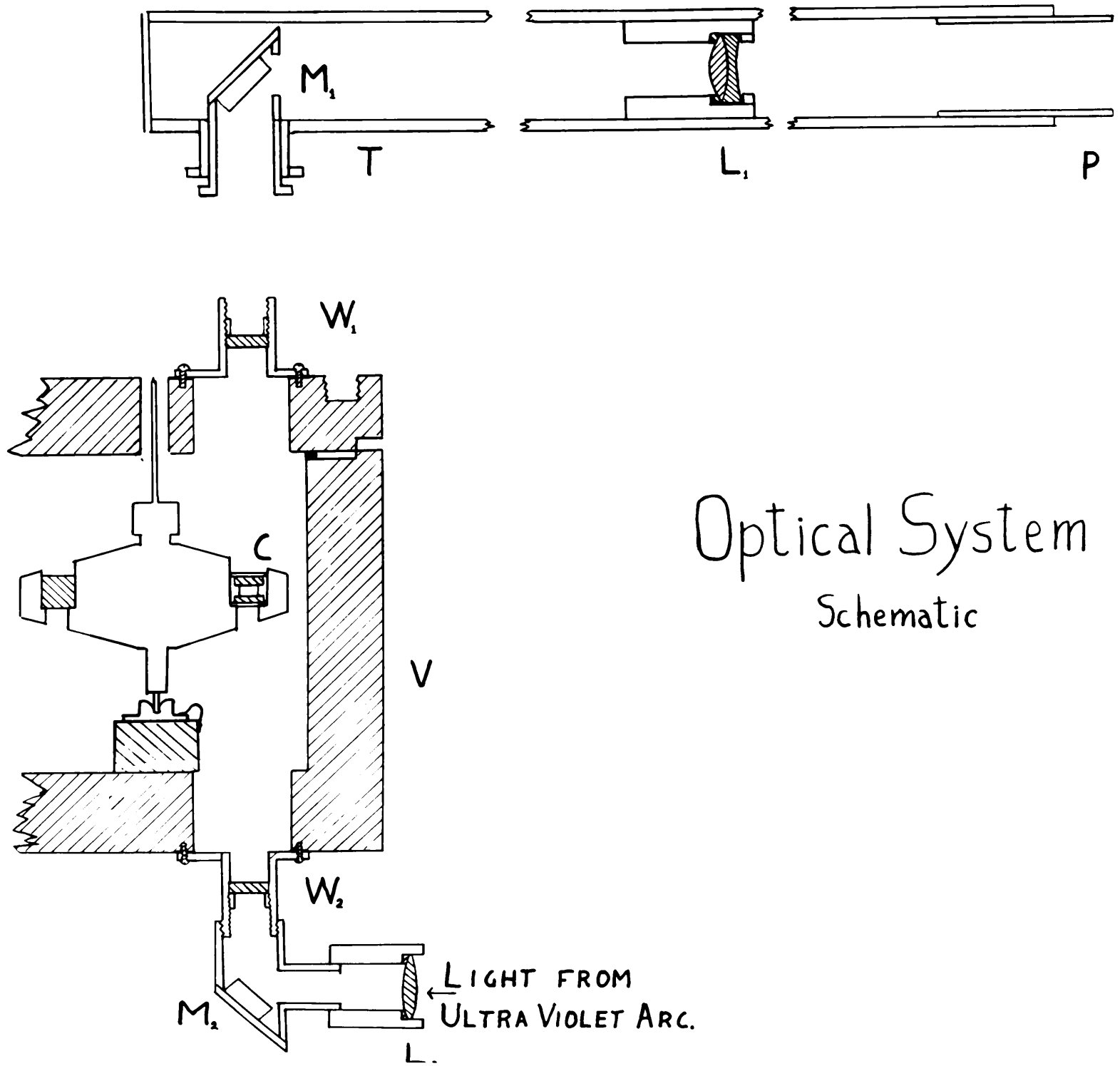

Optical System

Schematic

Svedberg[5] to be optimum; if the column of solution is too short there is insufficient space for sedimentation and molecules are reflected from the outer end of the space. For a given distance of the cell from the axis of rotation, the length of the cell space is limited by the phenomenon of inhomogeneity of the centrifugal field.

The centrepiece and quartz disks are held in an outer duralumin casing, A, of height 2.54 cm. and outer diameter 25.4 cm. and are clamped very tightly together by a clamping ring, K, which presses on the upper disk through the ring, L.

A seal is achieved between the disks and the centrepiece, through the use of pliofilm washers, H, 0.02 cm. thick, having an outer diameter of 1.9 cm. and an inner diameter of 1.5 cm. The seal is necessary to prevent leakage of the solution under the great hydrostatic pressure developed in the rotating cell. The pressure is 150 atmospheres at a speed of 800 revolutions per second.

The cell is filled through a small hole, E, in the centrepiece at the inner end of the sector. This hole is sealed, to prevent leakage by evaporation into the surrounding vacuum, by the pressure of a set screw, C, on a rubber washer, D, placed in an enlargement at the outer end of E.

Special wrenches, fitting into holes drilled in the bottom of the casing A and into the ring K, are used in tightening the cell. The amount of expansion of the casing, in the region of the threads, is used as a criterion of tightness.

In order to make the light beam through the cell accurately

CROSS-SECTION OF THE CELL

FIGURE 6

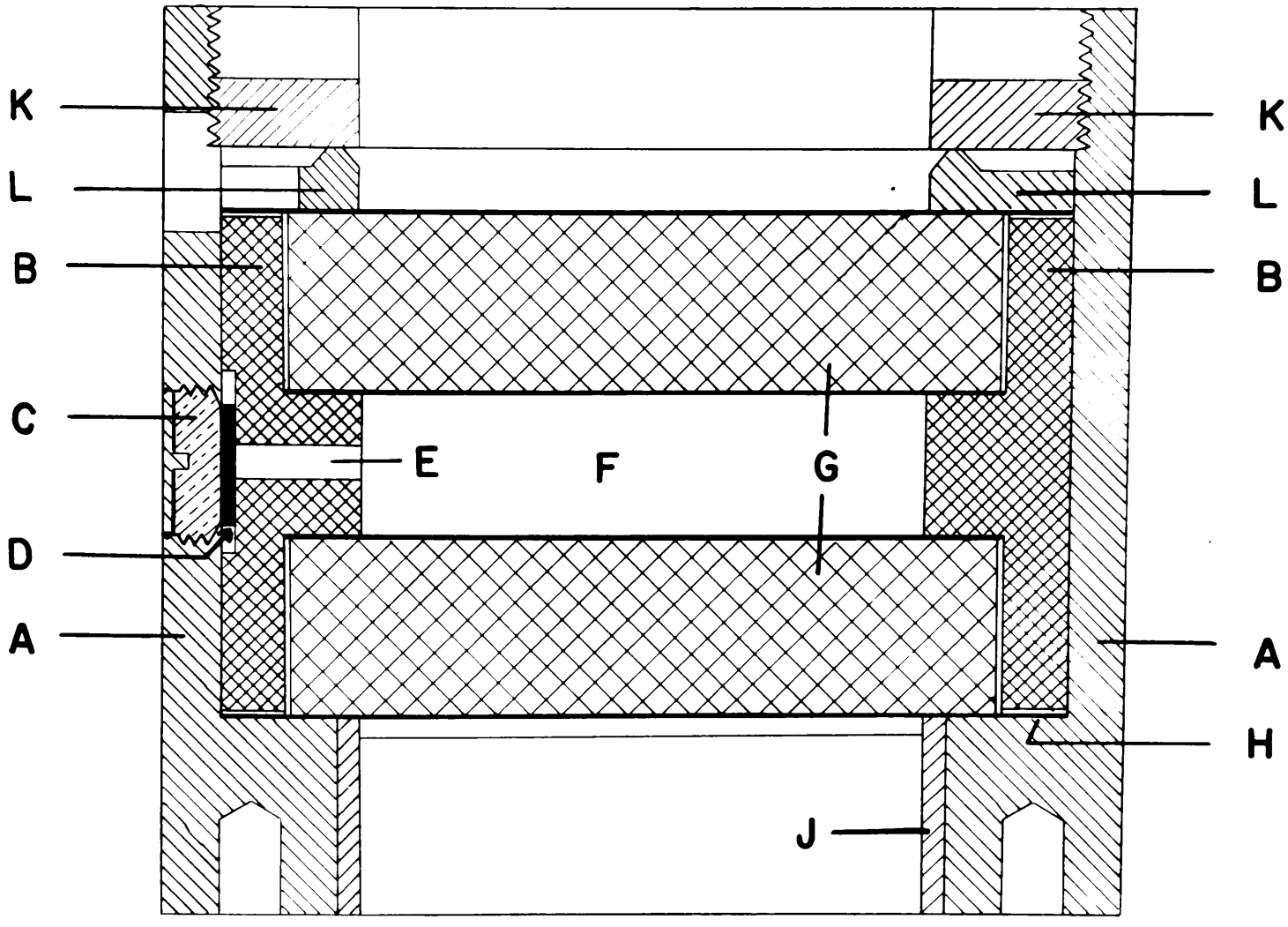
K
L
B
C
D
A
E
F
G
K
L
B
A
H
J

sector-shaped and hence to render the intensity of the light at the photographic plate independent of distance from the axis, a diaphragm, J, with an accurate sector-shaped opening of angular width 3 degrees, is placed in the bottom opening of the casing.

The first centrepiece used in the cell was made of a plastic, pontalite, as suggested by Bauer and Pickels.[20] When it was found, however, that the pressure of the set screw, C, necessary to seal the filling hole, was sufficient to crack the plastic about the hole, the present centrepiece of duralumin was adopted. The latter was given a dichromate coating to prevent chemical reaction with the cell contents. The recesses in the new centrepiece into which the quartz disks fit were made slightly large to allow for the insertion of double layers of pliofilm around the edges of the disks. The purpose of the compressible pliofilm layers is to reduce the stresses set up in the quartz disks by deformation during rotation of the cell, and, hence, to prevent fracture of the disks.

In use, the cell must be accurately aligned in the rotor, in order that the sectoral walls be along radii from the axis. Pickels[24] has suggested the use of a key fitting into corresponding slots in the rotor and the cell casing.

(b) <u>The Camera</u>

Another essential feature of the optical system is the camera lens, L_1. It is a Hilger quartz-fluorite achromatic doublet of focal length 100 cm. and aperture F 36. A long focus lens is

necessary to prevent errors due to parallax arising from the finite thickness of the column of solution in the cell. The lens is employed at unit magnification; thus the total length of the optical system from the cell to the image plane is 400 cm.

An aluminum camera tube, T, of inner diameter 5 cm. and length 315 cm., shown in Photographs 2 and 4, is rigidly supported at a height of 165 cm. above the floor of the room by wooden brackets built out from two brick pillars. The mounting of the camera lens in the tube has a rack and pinion adjustment for focussing.

A Hilger E_2 quartz spectrograph, with its slit placed in the image plane of the camera lens, serves instead of a photographic plate holder. The spectrograph has the immense advantage that it resolves light incident on it into a spectrum. The camera shutter is simply a wooden disk mounted to swing in front of and to fit closely against the spectrograph slit.

Light from the cell passes to the camera through the vacuum chamber window, W_1. This consists essentially of a quartz disk, identical with those used in the cell, which is mounted in a brass holder. A seal about W_1 is achieved by clamping it tightly against a shoulder of the holder with an interposed rubber gasket. A neoprene gasket provides a seal between the holder and the chamber lid.

A stainless steel mirror, M_1, mounted in the camera tube, changes the direction of light through 90 degrees. M_1 has an actual diameter of 2.4 cm. and an effective diameter of 1.7 cm.

Brass and aluminum tubes, shown in Photograph 2, enclose the light path from W_1 to M_1, excluding oil, dust and stray light. Diaphragms, placed in the tubes of the optical system at suitable intervals, reduce internal reflections.

(c) The Light Source

A General Electric 250 watt, 3 inch UViarc, a quartz mercury arc, is the source of visible and ultra-violet light (Photographs 2,3). Operating from the 110 volt A.C. lines through an autotransformer, this source provides illumination of constant intensity when it is fully warmed up. In operation, the lamp input voltage is carefully adjusted to a definite value with a Variac and a voltmeter. The warm-up period necessary is said to be 4 minutes; in operation a 6 minute period is allowed.

The cell is illuminated with parallel light from the mercury arc by means of the condenser lens, L_2, the mirror M_2 and the window W_2. L_2 is a quartz lens of focal length 25 cm. located at a distance of 25 cm. from the UViarc. M_2 and W_2 are identical with M_1 and W_1, respectively.

(d) Adjustment of the Optical System

Accurate alignment of the optical system is essential for the production of an evenly illuminated, focussed image of the cell. All of the components of the optical system are adjustable in their mountings to a sufficient degree to permit alignment.

(e) The Light Absorption Method

The light absorption method depends on the existence of a difference in absorption between the substance studied, and the medium surrounding it in the cell. In general, the medium or solvent is non-absorbing and the molecules or particles of the substance exhibit a characteristic absorption, usually in the ultraviolet. The use of a mercury arc source, unfiltered, and the spectrograph render unnecessary a search for the proper source frequency for a given substance and can extend the possibilities of the light absorption method by differentiating between two simultaneously sedimenting substances.

During a run, exposures are taken at certain intervals; on completion, a set of exposures is taken to determine the relation between blackening on the photographic plate and concentration of the sedimenting substance. The latter set provide what is known as the "concentration scale". After development, the exposed plates are registered with a microphotometer which yields a graph of photographic blackening against position in the cell.

(f) The Microphotometer

The microphotometer in use was manufactured by Kipp and Zonen. The principle of the instrument is as follows: An electric lamp is burned at a constant voltage, supplied by a storage battery. A reduced image of the lamp filament is projected through a lens on to the plate whose blackening is being registered. A second lens focusses this image on a thermopile whose current is measured by a Kipp galvanometer. The deflection of the latter is recorded with a

light beam, a mirror turned by the galvanometer and a strip of photographic paper on a drum. The drum and the plate are advanced together by a set of gears, such that a magnification of 7 is achieved on the drum. The resolution of the microphotometer is sufficient to show peaks on the photometric curves caused by the grains of the emulsion.

A small electric motor drives the photometer through a reduction gear, at such a speed that it traces over the complete cell image, 1.5 cm. in length, in 10 minutes. This rate is slow enough to permit the galvanometer to register accurately any sudden changes in blackening, e.g. that occurring at the meniscus in the cell.

The photographs taken in a run on the protein, egg albumin, are shown in Figure 9. Figure 10 is a microphotometer trace from this run. The blackening due to the "index", shown in Figure 10, is produced by allowing light to pass through a small hole in the cell counterbalance. This hole is located at an accurately known distance from the axis of rotation and its image furnishes a reference point for the measurement of displacements.

(g) Photographic Considerations

Kodak 33 plates, a general purpose, blue sensitive type, are used in the spectrograph, and are always developed for 3.5 minutes in Kodak developer D-19 at a temperature of $20^{\circ}C$.

The proper exposure time must be determined in advance of a run for a particular line of the mercury arc at which there is characteristic absorption by the solute of the solution being studied.

The exposure must be such that the concentrations of solution from 0% (pure solvent) up to 100% of the initial concentration in the cell at the beginning of the run, produce degrees of blackening, all of which lie on or near the linear portion of the photographic blackening curve of the plate.[5] That is, all of the concentrations to be observed in the cell, must produce different degrees of blackening on the plate, in order that an accurate relation between concentration and position in the cell may be obtained.

The effect of the phenomenon of growth of the latent image after exposure was eliminated by delaying development of the plates for a period long compared with the interval between the first and last exposures of a run.

The set of exposures from which the "concentration scale" is produced can be taken in two different ways. In the first, the cell is filled with a number of concentrations in the range from 0% to 100% and,for each concentration, an exposure is taken at the operating speed for the run. A second, simpler method involves the use of an optical cell, with parallel quartz windows separated by a distance equal to the ultracentrifuge cell thickness. During the run, the optical cell is filled with pure solvent, and is placed between light source and the ultracentrifuge cell. On completion of the run, when a region of pure solvent exists in the rotating cell, the optical cell is filled with a number of concentrations of the solution and an exposure is taken for each.

V. OPERATION OF THE ULTRACENTRIFUGE

Many details of operation are given by Rotenberg[23]; consequently, mention will be made only of some different phases encountered by the writer.

Some difficulty was experienced with the babbitt bearings. As mentioned above, the bearings should be reamed carefully until the shaft will just slide through without forcing. In practice, this is difficult to achieve; slightly tight bearings tend to seize and loose bearings experience a high rate of oil leakage. The outer diameter of the shaft material is actually 0.1263 inches. A special reamer, made by Mr. J. A. Massé, slightly smaller than this size, facilitated adjustment of the bearings. In Professor Beams' experience, such bearings do not wear if properly lubricated while the ultracentrifuge is running at a vibration-free speed; wear is caused by undesired reaming as the precessional vibration region is traversed in acceleration or deceleration.

In acceleration of the ultracentrifuge to the operating speed, the writer found, in agreement with Skarstrom and Beams[18], that the motor torque is roughly inversely proportional to drive frequency. Consequently, for a final speed of 800 revolutions per second, it is preferable to begin with the lowest available drive frequency, before changing to the final frequency.

The greatest speed at which the ultracentrifuge has been

run, 56,400 RPM or 940 revolutions per second, required 700 watts of driving power at a frequency of 1120 cycles per second. The earlier lighter Svedberg rotor was used at this speed, which corresponds to a field of 208,000 g. at the center of the cell.

No long runs were conducted at speeds greater than 800 revolutions per second; two at this speed lasted for 8 and 9 hours. They are described below under applications of the ultracentrifuge.

As mentioned above, the rotor may be brought rapidly to rest at the conclusion of a run, by reversing the current through one pair of stator coils. The application of 400 watts in reverse at 430 cycles per second results in a safe traversal of the precessional vibration region below 18,000 RPM.

The motor stator assumes a temperature above 70°C , during high speed runs, for which more than 500 watts of driving power are required. The blower, shown in Photograph 3, cools the stator effectively on one side. Further cooling was achieved by passing cold water through several turns of copper tubing around the outer edge of the stator. This system, although inefficient, maintains the stator everywhere within the safe temperature range.

During the early runs at high speed and high driving power, some of the phase shifting condensers shorted because of overheating. The difficulty was resolved by directing a steady flow of air over them with a blower and a 10-inch fan.

The water flow necessary to produce satisfactory cooling

in the armature-shaft assembly requires a pressure of 5 lbs., read on a gauge in the water inlet line. The lubricating oil pressure which must be higher than the water pressure, to prevent water from entering the babbitt bearings, is set, in general, at 10 lbs.

With the speed control, very little attention is required from the operator during a run, except for taking exposures and checking the oil and water pressures.

VI. THEORETICAL CONSIDERATIONS

A comprehensive treatment of the theory of sedimentation in a centrifugal field is given by Svedberg and Pedersen[5] and in briefer form by Beams.[26]

The theoretical problems involved have not yet been completely solved. The theory of Mason and Weaver[27] for sedimentation in ideal solutions in the gravitational field may be used for approximate results in centrifugation, where the centrifugal field can be considered uniform over the length of the cell. The differential equation, first derived by Lamm,[28] is

$$\frac{1}{x}\frac{\partial}{\partial x}\left\{\left(D\frac{\partial c}{\partial x} - \omega^2 xsc\right)x\right\} = \frac{\partial c}{\partial t} \qquad (1)$$

where c is the concentration at a point at time t of an ideal solution in a sector-shaped cell, rotating with constant angular velocity ω, x is the distance from the centre of rotation, D the diffusion constant and s the sedimentation constant, or the velocity of sedimentation of the solute in unit centrifugal field. Usable solutions of this equation have been obtained by Archibald,[29] by means of which theoretical distributions of concentration in the cell may be obtained for any time t. The simplest solution of the differential equation, that for the equilibrium case when $t = \infty$, has been given by Svedberg,[5] in the form

$$M = \frac{2RT \log_e c_1/c_2}{(1-V\rho)\omega^2(x_1^2 - x_2^2)} \qquad (2)$$

where M is the molecular weight, R the gas constant, T the absolute

temperature, ρ the density of the solution, V the partial specific volume of the substance and c_1 and c_2 the concentrations at points x_1 and x_2, respectively. At equilibrium, the opposing forces of sedimentation and diffusion balance one another. In practice, equilibrium may be approached sufficiently closely in a finite time, which is, however, in many cases, inconveniently long.

Another method, involving the measurement of sedimentation velocity, may be carried out in a comparatively short time, with a sufficiently high centrifugal field. The theory of the method may be developed as follows: The centrifugal force on acting on N particles suspended in a fluid is

$$N\phi(\rho_p - \rho)\omega^2 x$$

where ϕ is the volume of one particle, ρ_p is the particle density and ρ is the density of the liquid. If N is Avogadro's number, then

$$N\phi\rho_p = M \quad \text{and} \quad N\phi\rho = MV\rho$$

where V is the partial specific volume of the solute. The frictional force acting on the mole of particles is

$$f\,\frac{dx}{dt}$$

where f is the frictional constant per mole. Equating the two forces, we have

$$M(1-V\rho)\omega^2 x = f\,\frac{dx}{dt}$$

For a dilute solution

$$f = \frac{RT}{D}$$

If we assume that the same molar frictional constant is effective in free diffusion and in sedimentation, then

$$M = \frac{RT}{D(1-V\rho)} \quad \frac{\frac{dx}{dt}}{\omega^2 x}$$

$$= \frac{RTs}{D(1-V\rho)} \qquad (3)$$

where s, the sedimentation constant, is a characteristic constant of a given molecular species in a given solvent at a given temperature.

Equations (2) and (3) are the two fundamental relations for centrifugal sedimentation. Equation (3) requires a knowledge of the diffusion constant for a determination of the molecular size. For many purposes, however, the sedimentation constant is a sufficient measure of molecular size. A comparison of M values using the two fundamental relations has revealed no systematic deviation, thus the assumptions made seem justified.

The sedimentation velocity method, however, has a much greater ability to analyze a mixture of molecular weights and this property is one of the major advantages of the ultracentrifuge over the osmotic pressure method.

A solution having a sdute with only one molecular species is known as monodisperse; a mixture containing a great number or a continuous series of molecular or particle species is polydisperse. The monodisperse system in sedimentation exhibits a very definite boundary between the solution and the pure solvent.

The simplest case of analysis of polydisperse systems by the sedimentation velocity method is when the particles are approxi-

mately spherical and large enough that no appreciable amount of diffusion takes place during the sedimentation measurements. The method of analysis of this case is described by Kraemer.[30] In the absence of interaction due to electric charge or too high a concentration, each particle size sediments with a sharp boundary, at a velocity given by Stokes' law. The law has the form for a sphere sedimenting in a fluid under the gravitational field:

$$r^2 = \frac{9\eta \frac{dx}{dt}}{2(\rho_p - \rho_m) g}$$

where $\frac{dx}{dt}$ is the velocity of the particle, η the viscosity of the medium, ρ_p the particle density, ρ_m the density of the medium, and g the gravitational field. In applying the equation to a centrifugal field $\omega^2 x$ is substituted for g, and the result, after integration is

$$r^2 = \frac{9\eta \log(\frac{x_t}{x_o})}{2(\rho_p - \rho_m)\omega^2 t}$$

where x_t is the distance of the particle from the axis of rotation at time t after the start of centrifugation and x_o is the distance of the meniscus from the axis. If the medium is more dense than the particle, as is the case with synthetic rubber latices in aqueous suspensions, then the latter sediments toward the axis and the relation becomes

$$r^2 = \frac{9\eta \log(\frac{x_p}{x_t})}{2(\rho_m - \rho_p)\omega^2 t} \qquad (4)$$

where x_p is the distance of the outer periphery of the cell from the axis of rotation.

After sedimentation for a time t, the increase in concentration dc_t over the region x_t to $(x_t - d_x)$ in the sedimenting boundary is due to particles of radius between r and $(r+dr)$ whose boundaries lie in this region. Owing to radial sedimentation and to the increase of centrifugal force with distance from the axis, the concentration of the group of particles at the outer periphery, in the original solution was less by the factor $\left(\frac{x_t}{x_p}\right)^2$

Then $$\frac{dc}{dx} = \frac{dc_t}{dx}\left(\frac{x_t}{x_p}\right)^2$$

A convenient method of representing the size-distribution of a mixture of spherical particles is by means of a plot of $\frac{dc}{dr}$ against r.

From equation (4)

$$\frac{dr}{dx} = -\frac{r}{2x_t \log\left\{\frac{x_p}{x_t}\right\}}$$

The negative sign indicates that the radius decreases as distance of the particle from the axis increases.

Then

$$\frac{dc}{dr} = \left(\frac{x_t}{x_p}\right)^2 \frac{dc_t}{dx}\,\frac{dx}{dr}$$

$$= -\frac{dc_t}{dx}\,\frac{2(x_t)^3}{rx_p^2}\log\left(\frac{x_p}{x_t}\right) \qquad (5)$$

For mixtures with very many components differing very slightly in particle size, the boundaries of the individual sizes do not appear in the sedimentation diagram and an analysis by means of equation (5) must be carried out in steps over the boundary.

Since dispersions with particles large enough to allow this simple analysis are usually turbid, the absorption method often is the only one which can be employed, the absorption being due to scattering. Scattering, however, is quite sensitive to differences in particle size, and the distribution curves as obtained above are really distributions of $\frac{d(kc)}{dr}$, where k is the absorption coefficient. Such curves are called weight-optical curves.

Rinde[31] has shown that if the particles are not perfect spheres, the ratio of the equivalent radius, obtained by Stokes' law to the radius R of the sphere of the same volume as the particle does not deviate far from unity, even if the particle is an ellipsoid with a ratio of axes of 10.

Size distribution analysis can be carried out by this procedure, ignoring diffusion for particles from approximately 100 A^{o} in diameter up to the sizes handled by sieve analysis.

PICK-UP COIL

FIGURE 7

CELL CENTREPIECE

FIGURE 8

EGG ALBUMIN RUN

PHOTOGRAPHS

FIGURE 9

MICROPHOTOMETER TRACE

FIGURE 10

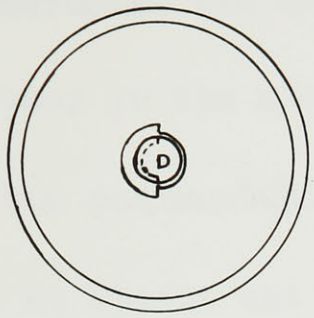

Pick-up Coil
Plan

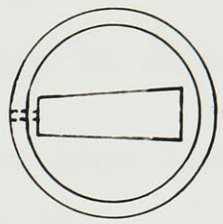

Cell Centrepiece
Plan

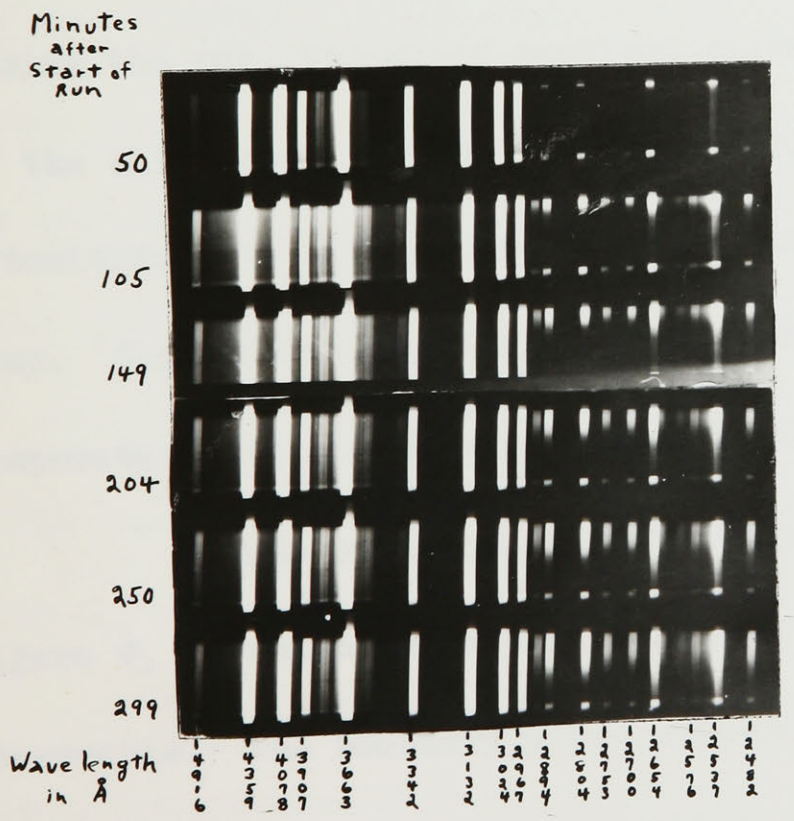

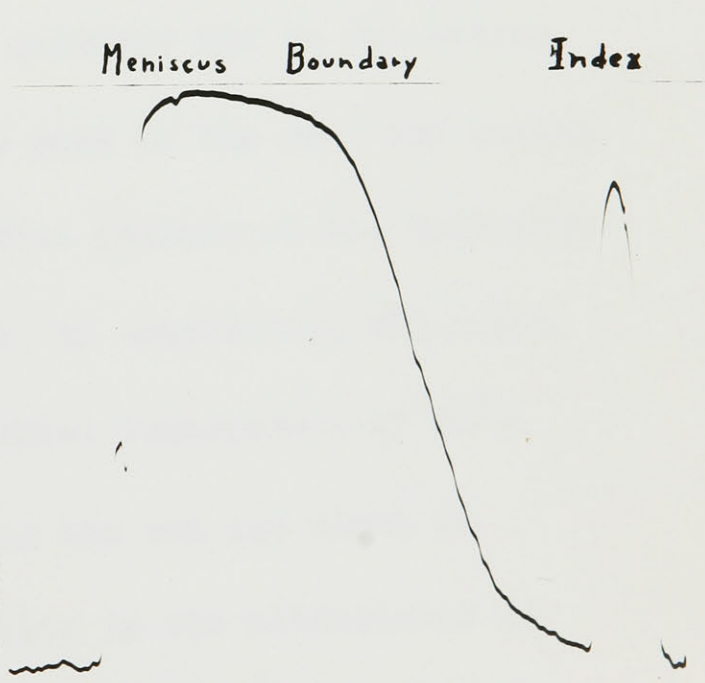

Microphotometer Trace - λ 2804 - 299 min

EGG ALBUMIN RUN

VII. APPLICATIONS

(a) The Sedimentation Constant of Egg Albumin.

The first measurement was made on the protein, egg albumin, a substance whose behaviour in the ultracentrifuge is well-known. Many determinations of its sedimentation constant have been made in Svedberg's laboratories at Upsala and elsewhere.[5,26]

A solution of Merck Egg albumin of concentration 1% by weight in water, was centrifuged for 5 hours at a speed of 700 revolutions per second or a centrifugal field at the cell centre of 113,000 g. Exposures were taken at intervals of 50 minutes, roughly. During the run, the speed remained quite constant due to the action of the slip speed control. In the latter part of the run, the vacuum deteriorated to 10 microns, owing to partial failure of the diffusion pump. Some heating of the rotor resulted; on completion, the rotor temperature had risen to 31°C from an initial temperature of 25°C.

Prints of exposures taken during the run are shown in Figure 9, in which characteristic absorption in the ultraviolet is observable. The boundary moves outward from the meniscus, since the protein molecules are more dense than the solvent. Figure 10 is a microphotometer trace from this run, of the λ2804 line, 299 minutes after the start. No concentration scale was made, owing to the lack of a suitable optical cell.

An evaluation of the sedimentation constant for this run yields the value 3.8×10^{-13}. The accepted value at 20°C, given by Svedberg and Pedersen[5] is 3.55×10^{-13}.

(b) Soap Solutions

The state of soap, commonly the sodium or potassium salt of a fatty acid, in aqueous solution is not definitely known. It is assumed, however, that the soap molecules are aggregated, above a certain minimum concentration of the solution, into micelles. A definitely known feature of the micelle is that soap molecules are oriented in pairs with the hydrocarbon ends together and the metal ion ends outward. It is assumed that the pairs are situated adjacent to one another in an aggregation resembling a "pancake", which may contain two or three hundred molecules. A layer of water is bound inside the "pancake". Harkins[32] has obtained this picture of the micelle from X-ray diffraction studies. Micelle formation occurs only above a certain minimum or critical concentration, about 0.1% by weight.

Soap is an essential factor in the polymerization process used to manufacture GR-S synthetic rubber. Polymerization occurs in an emulsion consisting of an oil phase and an aqueous phase. The oil phase consists principally of butadiene and styrene in proportions dependent on the properties desired in the final product; the aqueous phase consists essentially of a soap solution. Polymerization

is pictured as being initiated within the micelle, which, in the emulsion, absorbs some of the oil phase. The yield of polymer from the reaction is sensitive to the amount and nature of the soap used. Some of the commercial soaps employed produce high yields; whereas, others are inefficient. It has been impossible on the basis of chemical analysis to determine what is the characteristic of a soap determining its efficiency in the reaction. If the nature of the micelle were known, more definitely, correlation of micelle structure with the mechanism of emulsion polymerization might be possible.

Dr. J. S. Tapp of the Research and Development Division of the Polymer Corporation suggested that the ultracentrifugal technique might reveal something of micelle structure. Three samples were supplied by Dr. Tapp: one was a standard soap, known to produce good yields; the other two were unsatisfactory soaps.

The sedimentation of soap in aqueous solution has been investigated by J.W. McBain and M.E.L. McBain[33], using the first oil-turbine ultracentrifuge built by Svedberg at Upsala. At a field of 100,000 g. several types of pure soaps, among them sodium oleate, potassium laurate and lauryl sulphonic acid, were centrifuged in concentrations of 0.25N and 0.5N, corresponding to percentages by weight of approximately 7.5% and 15%. Using the light absorption method, sedimentation was observed to take place outward with potassium laurate and inward with sodium oleate and lauryl sulphonic acid. McBain and McBain ascribed the outward sedimentation to an "ionic"

micelle, that inward to a neutral micelle. The results could not be evaluated because the absorption of light was found to be independent of concentration in the middle of the concentration range.

The standard RRC Pilot Plant soap was selected for preliminary experiments. Concentrations above 0.5% proved impractical owing to gel formation. A number of runs with solutions of concentration 0.25%, including one of 9 hours at 113,000 g., were conducted, with no observable sedimentation. A later run of 9 hours duration at 150,000 g., disclosed some slight sedimentation inward to the meniscus. This corresponds somewhat to the result obtained by the McBains with sodium oleate at a concentration of about 7.5%, much greater than that used here.

At this point in the investigation of soaps, when runs on pure soaps were contemplated, the accident with the earlier Svedberg rotor occurred. Owing to a lack of time, the soap problem was deferred and the experiments described below were undertaken.

(c) Particle Size Distributions in GR-S Synthetic Rubber Latices.

Synthetic rubber latex, the end product of the polymerization reaction, consists of rubber particles in an aqueous suspension. The particles, have particle weights near $\bar{1}0^8$ grams and diameters near 500 A°. Measurements of latex particle sizes and distributions are of fundamental importance in establishing both the locus and the mechanism of the emulsion polymerization process. They have been made previously by the use of three

different methods; (a) light scattering techniques (b) the determination of specific area and size by soap titration (c) the use of the electron microscope. A comprehensive summary of these three methods has been given by M.L. Corrin.[34] Even after correction of the results for the different methods of averaging in use, the three methods yield different results.

The order of size of the latex particle makes it particularly suitable for employment of the theory described above for polydisperse systems, in which sedimentation is sufficiently rapid that diffusion may be neglected.

Two samples of latex, types II and V were supplied by the Polymer Corporation. Type II is the latex produced in normal manufacture, and has particle sizes predominantly in the "small" end of the latex particle size range. Type V is said to have larger particles. The latex samples are highly turbid and for use must be greatly diluted. A 0.1% solution of the standard Pilot soap was used for the dilution which was 1:1000 for Type II and 1:2000 for Type V, corresponding to percentage concentrations by weight of 0.025% and 0.029%, respectively. Bardwell and Sivertz[35] have found that a soap solution is necessary for the dilution, rather than water, in order to prevent agglomeration of the latex particles. At these great dilutions, which were selected to provide proper photographic exposures in the ultracentrifuge, a definite turbidity is nevertheless noticeable. Test runs to determine the proper centrifuge speed, revealed that 5500 RPM corresponding to a field in the cell of 1960 g was suitable.

The run on Type II latex lasted 3 hours; during the run exposures were taken at 18 minutes and 30 minutes after the start and at 25 minute intervals thereafter. A concentration scale was made at the

conclusion of the run by filling the cell successively with concentrations of 0,20,40,60,80 and 100% of the initial concentration and taking an exposure for each concentration at 5500 RPM. Microphotometer traces were made of the λ 2654 line which proved to be well exposed. The exposure at 30 minutes was selected for analysis because of its region of uniform concentration between the meniscus and the boundary. A curve corresponding to the boundary, giving microphotometer deflection versus distance from the axis of rotation is shown in Figure 11.

The results are analyzed as follows: from the microphotometer trace, corresponding values of displacement of points of the boundary from the index and photometer deflection are obtained. The distances from the index are converted to distances from the axis of rotation and the graph mentioned above in Figure 11 is plotted. Photometer deflections are changed by means of the concentration scale (Figure 11) to concentration values. These quantities above are tabulated, along with corresponding values worked out for the following: $\left(\frac{x_p}{x_t}\right)$, $\left(\frac{x_p}{x_t}\right)^2$, log $\left(\frac{x_p}{x_t}\right)$, r^2, r, Δr, r_m, Δr_o, Δc_t, $\frac{\Delta c_t}{\Delta r_o}$, where Δr and Δc_t represent the differences between successive values of r and c_t; r_m is the mean radius in the corresponding interval; Δr_o carries the correction for bunching and is $\Delta r \left(\frac{x_p}{x_t}\right)^2$. $\frac{\Delta c_t}{\Delta r_o}$ is equal to $\frac{\Delta c}{\Delta r}$ and is the ordinate of the size distribution function plotted against r_m as abscissa. Values of r^2 are calculated with equation (4) of the theory. The distribution curve for the Type II latex is shown in Figure 11.

The run on Type V latex was conducted similarly. The λ 2804 line was chosen and a concentration scale constructed. An exposure taken 18 minutes after the beginning of the run was analysed as described above. The results are shown in Figure 12.

The measurements of viscosity of the latex solutions and of the density of the medium (soap solution) necessary to supply values for the calculation of r^2, were made through the kindness of Professor Winkler in his laboratory. The values are as follows:

Viscosity of Type II Latex solution - 9.45×10^{-3} poises

Viscosity of Type V Latex solution - 9.22×10^{-3} poises

Density of 0.1% soap solution - 0.997 g./litre.

Bardwell and Sivertz[35] have determined the density of the latex particles to be 0.93 g./litre, the same as the accepted density of the bulk polymer.

The size distribution curves, which are weight-optical curves, as mentioned above, indicate distribution in accordance with the anticipated results. The significance of the curves is such that an average particle radius, which may be called a weight-optical average, is given by the radius coordinate of the centre of gravity of the distribution curve, calculated from the formula:

$$r_{av} = \frac{\int_0^{\infty} r \frac{d(kc)}{dr} dr}{\int_0^{\infty} \frac{d(kc)}{dr} dr}$$

Calculations of r_{av} yield the values: 590 A° for Type II and 940 A° for Type V. The value for Type II lies near the average value, 560 A° determined by light scattering measurements.[34]

B I B L I O G R A P H Y

1. Perrin, Compt. Rend. 146, 967, 1908.
2. Dumansky, Kolloid-Z. 12, 6, 1913.
3. Svedberg and Rinde, J.Am. Chem.Soc. 45, 943, 1923.
4. Svedberg and Nichols, J.Am. Chem. Soc. 45, 2910, 1923.
5. Svedberg and Pedersen, "The Ultracentrifuge", Oxford University Press, 1940.
6. Henriot and Huguenard, Compt. Rend. 180, 1389, 1925.
7. Beams, Rev. Sci. Inst., 1, 667, 1930.
8. Beams, Weed and Pickels, Science 78, 338, 1933.
9. Pickels and Beams, Phys. Rev. 47, 336, 1935.
10. Beams and Pickels, Rev. Sci. Inst. 6, 299, 1935.
11. McBain and O'Sullivan, J.Am. Chem. Soc. 57, 780 and 2631, 1935.
12. McBain and Alvarez-Tostado, J.Am. Chem. Soc. 59, 2489, 1937.
13. McBain and Leyda, J.Am. Chem. Soc. 60, 2998, 1938.
14. McBain, J.Phys. Chem. 42, 1063, 1938.
15. McBain and Lewis, J.Phys. Chem. 43, 1197, 1939.
16. Beams and Snoddy, Science 85, 185, 1937.
17. Beams and Black, Rev. Sci. Inst. 10, 59, 1939.
18. Skarstrom and Beams, Rev. Sci. Inst. 11, 398, 1940.
19. Bauer and Pickels, J. Exp. Med. 64, 503, 1936.
20. Bauer and Pickels, J. Exp. Med. 65, 565, 1937.
21. Pickels, Rev.Sci.Inst. 9, 358, 1938.
22. Brunetti, Rev.Sci.Inst. 10, 85, 1939.
23. Rotenberg, "An Electrically Driven Ultracentrifuge", McGill Thesis, 1941.

24. Pickels, Rev.Sci.Inst. 13, 426, 1942.

25. Svedberg and Nichols, J.Am.Chem.Soc. 48, 430, 1926.

26. Beams, Rev. Mod. Phys. 10, 245, 1938.

27. Mason and Weaver, Phys.Rev. 23, 412, 1924.

28. Lamm, Arkiv Math.Astron.Fysik 21B, No. 2, 1929.
Zeits.f.physik.Chemie 143A, 177, 1929.

29. Archibald, Phys. Rev. 53, 746, 1938; 54, 371, 1938;
J.App.Phys. 18, 362, 1947.

30. Kraemer, page 325 of Reference 5.

31. Rinde, Dissertation, Upsala, 1928.

32. Harkins, J.Am.Chem.Soc. 68, 220, 1946;
J. Colloid Science 1, 105, 1946.

33. McBain, J.W. and McBain, M.E.L., Proc.Roy.Soc. 139A, 26, 1933.

34. Corrin, Technical report to the Office of Rubber Reserve,
CR-1417, April, 1947.

35. Bardwell and Sivertz, Can.Jour.Res. 25B, 255, 1947.

TYPE II LATEX RESULTS

FIGURE 11

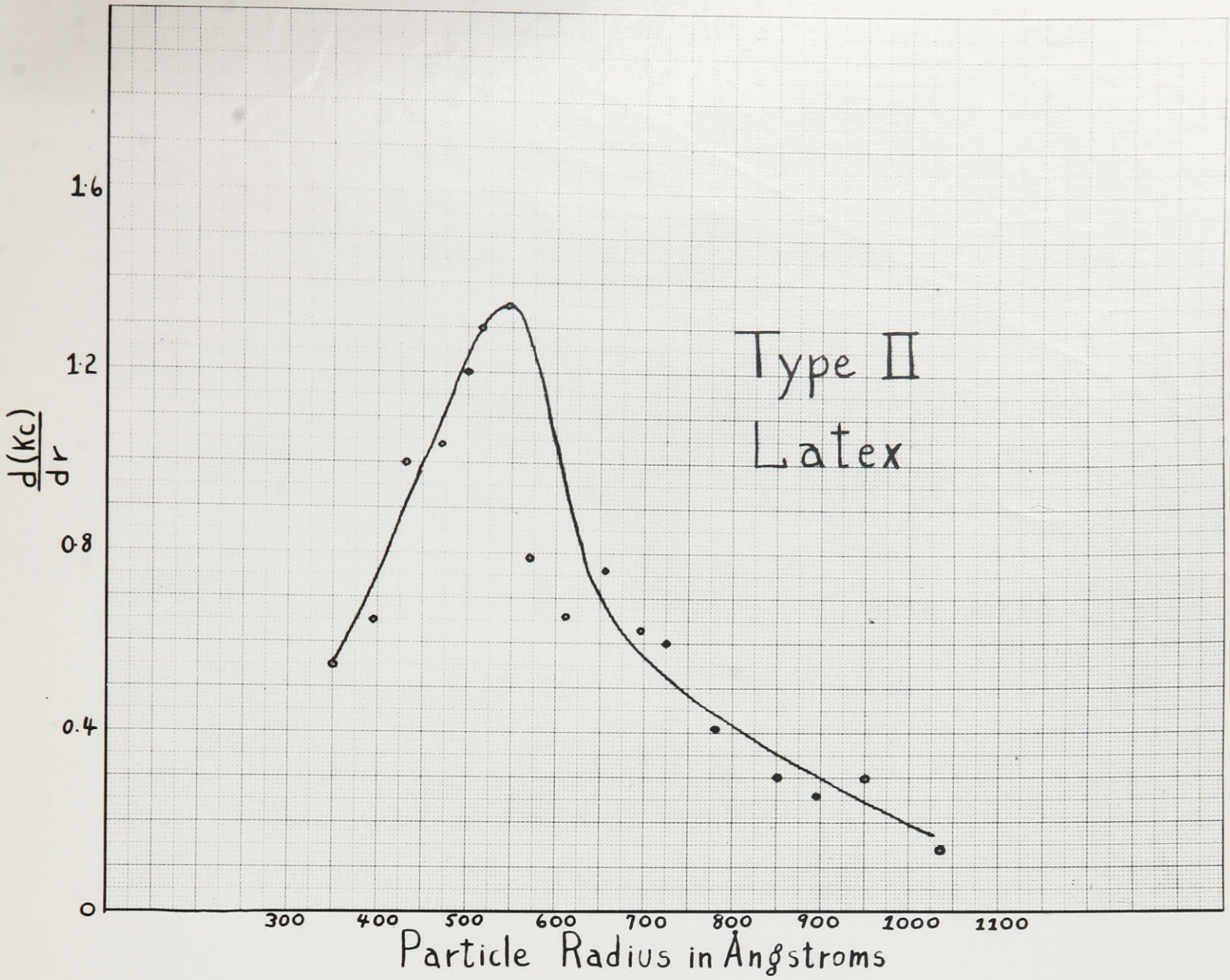
Type II
Latex
d(Kc)/dr
1.6
1.2
0.8
0.4
0
300
400
500
600
700
800
900
1000
1100
Particle Radius in Angstroms

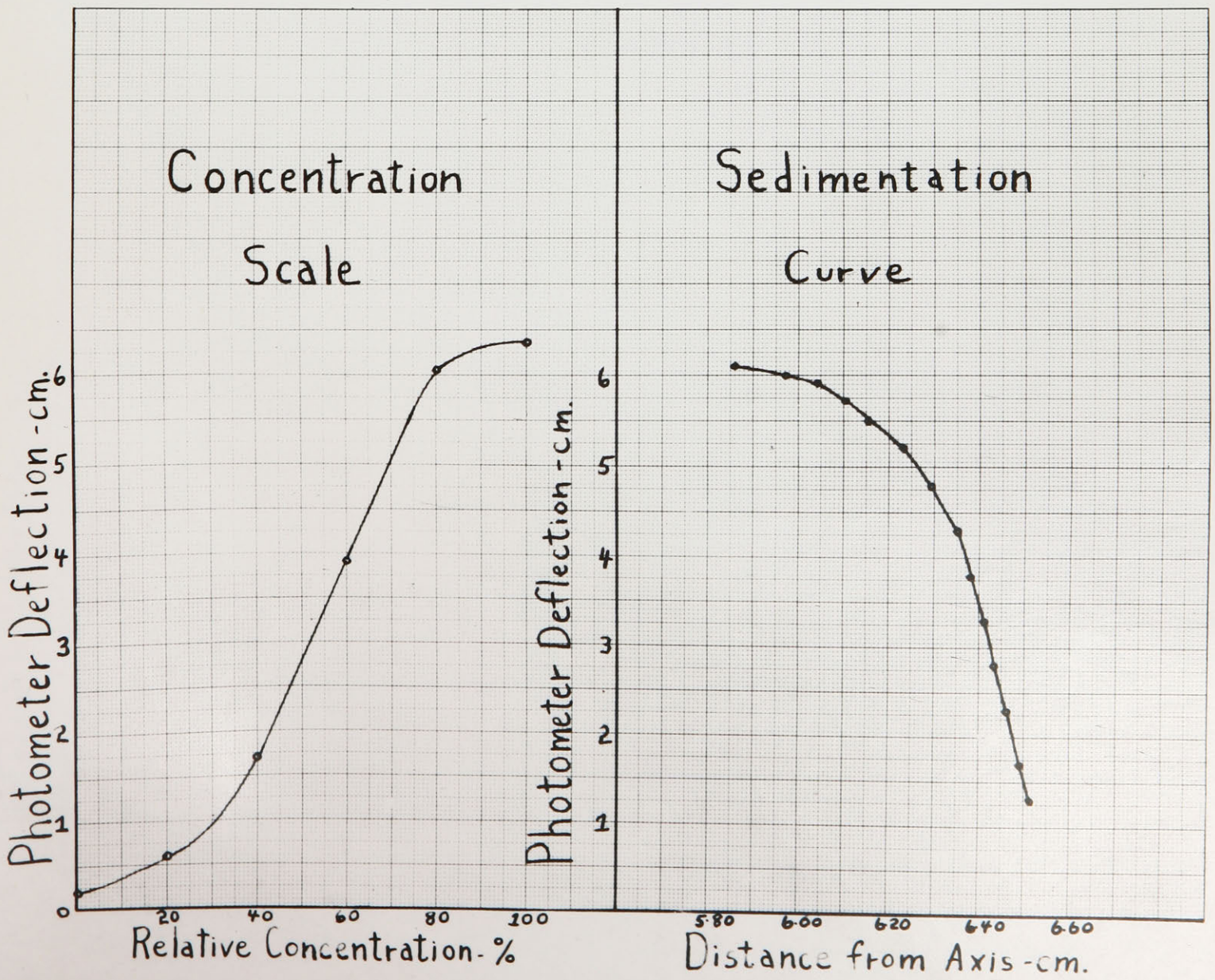
Concentration
Scale
Photometer Deflection - cm.
0
1
2
3
4
5
6
20
40
60
80
100
Relative Concentration - %
Sedimentation
Curve
Photometer Deflection - cm.
5.80
6.00
6.20
6.40
6.60
Distance from Axis - cm.

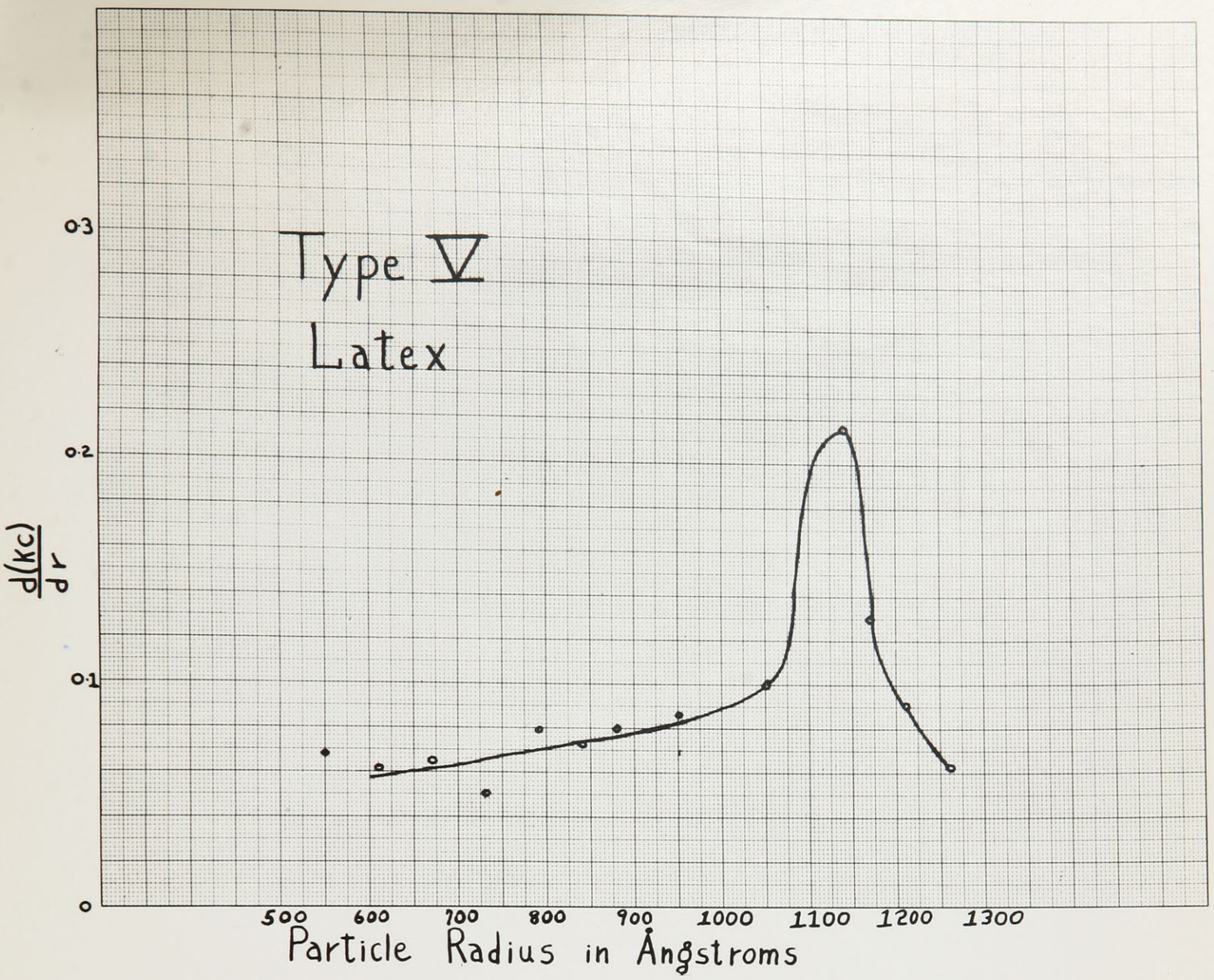
Type V
Latex
d(kc)/dr
0
0.1
0.2
0.3
500
600
700
800
900
1000
1100
1200
1300
Particle Radius in Ångstroms

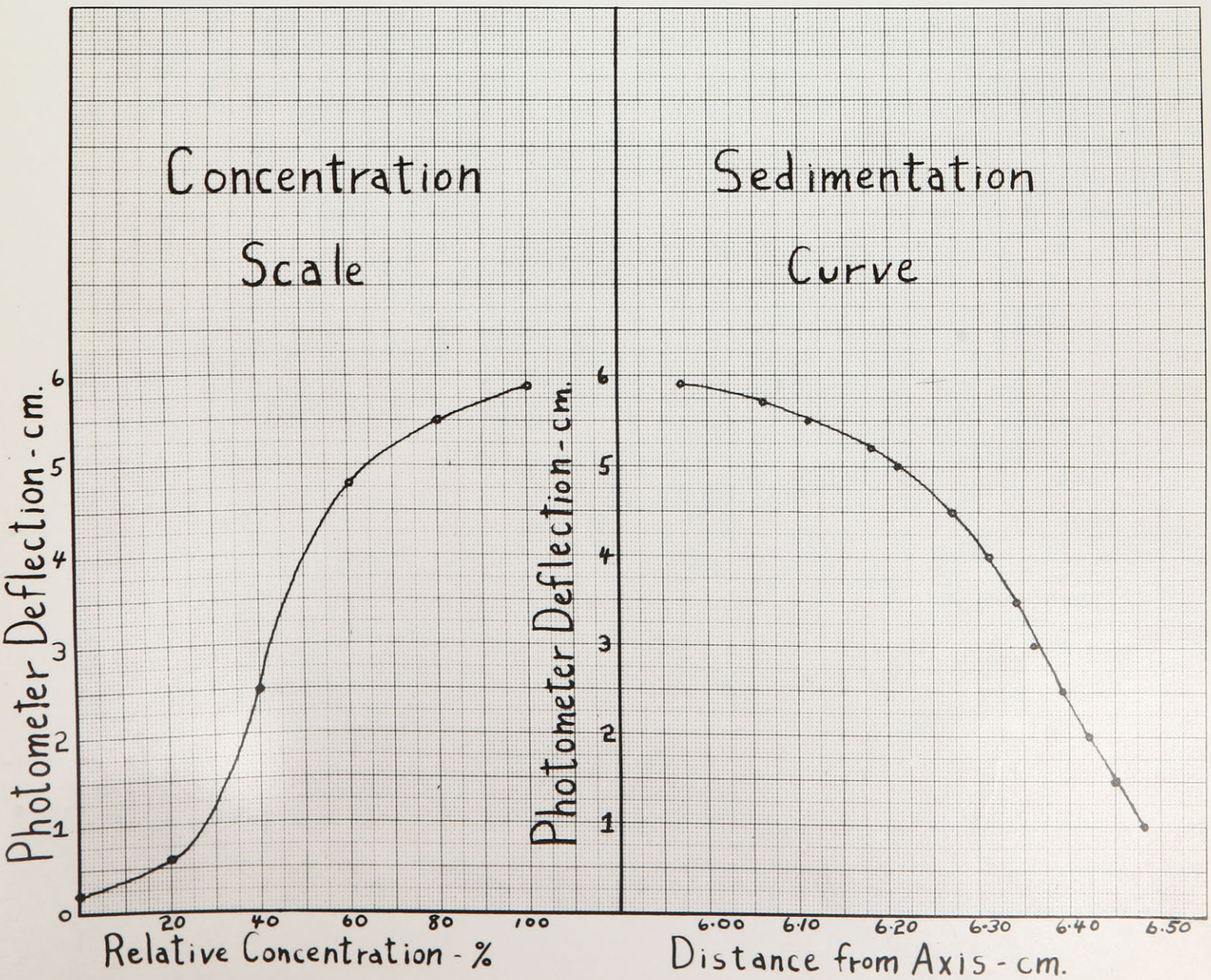
Concentration
Scale
Sedimentation
Curve
Photometer Deflection - cm.
0
1
2
3
4
5
6
20
40
60
80
100
Relative Concentration - %
6.00
6.10
6.20
6.30
6.40
6.50
Distance from Axis - cm.

PHOTOGRAPH 1.

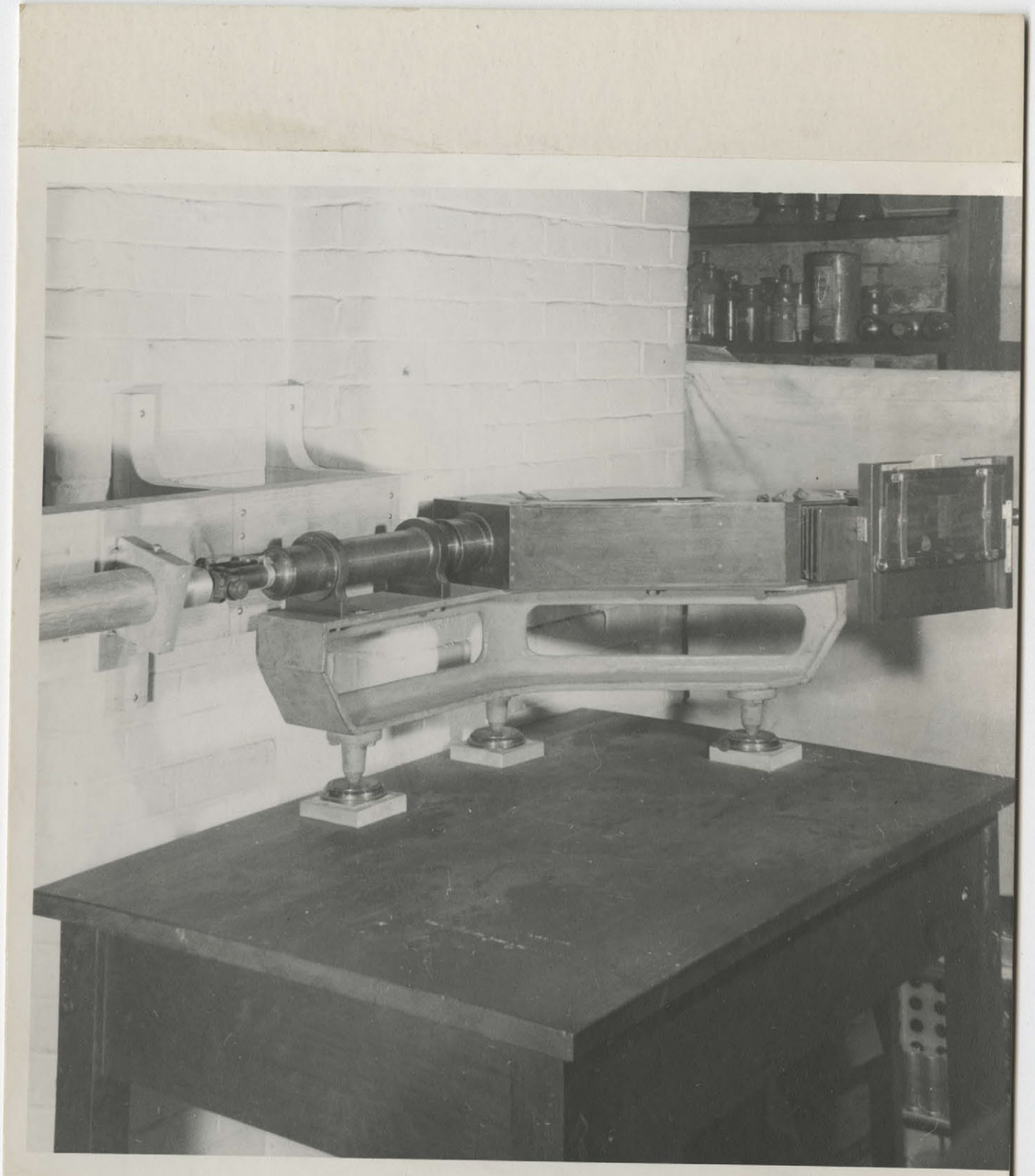

PHOTOGRAPH 2.

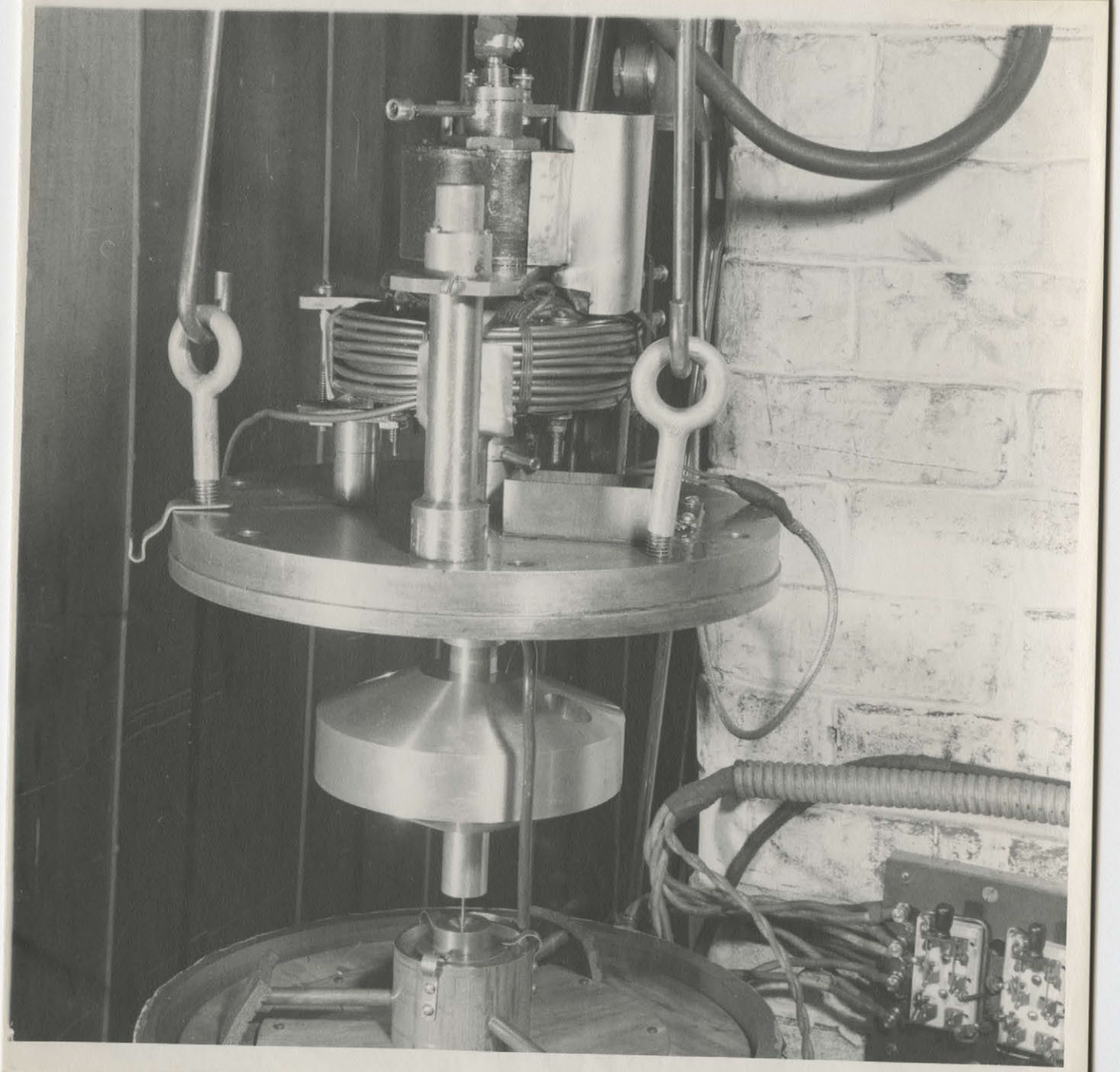

PHOTOGRAPH 3.

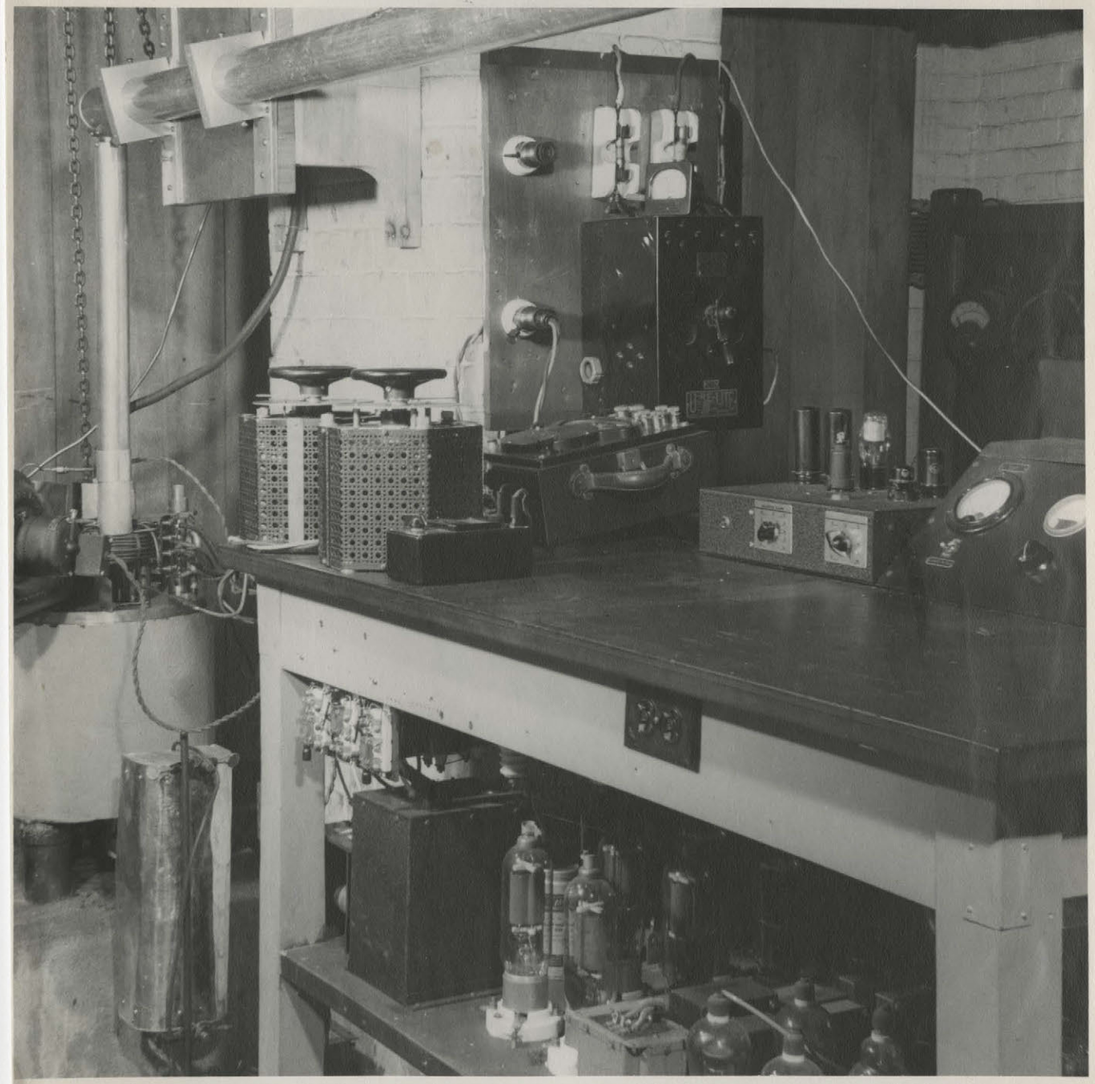

PHOTOGRAPH 4.